

## Predicting illness trajectory and hospital resource utilization of COVID-19 hospitalized patients – a nationwide study

Michael Roimi<sup>1,\*</sup>, Rom Gutman<sup>2,\*</sup>, Jonathan Somer<sup>2</sup>, Asaf Ben Arie<sup>3</sup>, Ido Calman, Yaron Bar-Lavie<sup>1</sup>, Arnona Ziv<sup>4</sup>, Danny Eytan<sup>1,2</sup>, Malka Gorfine<sup>3,\*\*</sup>, Uri Shalit<sup>2,\*\*</sup>

---

### Abstract

**Importance** The spread of COVID-19 has led to a severe strain on hospital capacity in many countries. There is a need for a model to help planners assess expected COVID-19 hospital resource utilization.

**Objective** Provide publicly available tools for predicting future hospital-bed utilization given a succinct characterization of the status of currently hospitalized patients and scenarios for future incoming patients.

**Design** Retrospective cohort study following the day-by-day clinical status of all hospitalized COVID-19 patients in Israel from March 1st to May 2nd, 2020. Patient clinical course was modelled with a machine learning approach based on a set of multistate Cox regression-based models with adjustments for right censoring, recurrent events, competing events, left truncation, and time-dependent covariates. The model predicts the patient's entire disease course in terms of clinical states, from which we derive the patient's hospital length-of-stay, length-of-stay in critical state, risk of in-hospital mortality, and overall hospital-bed utilization. Accuracy assessed over 8 cross-validation cohorts of size 330, using per-day Mean Absolute Error (MAE) of predicted hospital utilization over time; and area under the receiver operating

---

\*Joint first authors

\*\*Joint last authors and corresponding authors, [gorfinem@tauex.tau.ac.il](mailto:gorfinem@tauex.tau.ac.il), [urishalit@technion.ac.il](mailto:urishalit@technion.ac.il)

<sup>1</sup>Rambam Health Care Campus

<sup>2</sup>Technion - Israel Institute of Technology

<sup>3</sup>Tel Aviv University

<sup>4</sup>The Gertner Institute for Epidemiology and Health Policy Research

characteristics (AUROC) for individual risk of critical illness and in-hospital mortality, assessed on the first day of hospitalization. We present predicted hospital utilization under hypothetical incoming patient scenarios.

**Setting** 27 Israeli hospitals.

**Participants** During the study period, 2,703 confirmed COVID-19 patients were hospitalized in Israel for 1 day or more; 28 were excluded due to missing age or sex; the remaining 2,675 patients were included in the analysis.

**Main Outcomes and Measures** Primary outcome: per-day estimate of total number of hospitalized patients and number of patients in critical state; secondary outcome: risk of a single patient experiencing critical illness or in-hospital mortality.

**Results** For random validation samples of 330 patients, the per-day MAEs for total hospital-bed utilization and critical-bed utilization, averaged over 64 days, were  $4.72 \pm 1.07$  and  $1.68 \pm 0.40$  respectively; the AUROCs for prediction of the probabilities of critical illness and in-hospital mortality were  $0.88 \pm 0.04$  and  $0.96 \pm 0.04$ , respectively. We further present the impact of several scenarios of patient influx on healthcare system utilization, demonstrating the ability to accurately plan ahead how to allocate healthcare resources.

**Conclusions and Relevance** We developed a model that, given basic easily obtained data as input, accurately predicts total and critical care hospital utilization. The model enables evaluating the impact of various patient influx scenarios on hospital utilization. Accurate predictions are also given for individual patients' probability of in-hospital mortality and critical illness. We further provide an R [software package](#) and a [web-application](#) for the model.

---

## 1. Introduction

2 The coronavirus disease 2019 (COVID-19) was first recognized in Wuhan,  
3 China in December 2019. On March 11 2020 the world health organization  
4 characterized the disease as a pandemic [1]. Worldwide, the COVID-19 pan-  
5 demic poses a major challenge for the healthcare systems and it will probably  
6 continue to pose challenges in the coming years [2, 3]. In particular, the dis-  
7 ease has taken its toll on healthcare systems around the world with some  
8 patients requiring lengthy general and intensive care [4].

9 Given the danger of unprecedented burden on healthcare systems due to  
10 COVID-19, there is a need for tools that help decision-makers plan resource  
11 allocation on the unit, hospital, regional and national levels. In this study

12 we aimed to use a nationwide hospitalization registry which includes the  
13 day-by-day hospitalization record of all the confirmed COVID-19 patients in  
14 Israel.

15 We used the registry to develop a tool for accurate projections of the  
16 total number of hospitalized patients and critical-care occupancy based on  
17 the state of the current hospitalized patient population and projections of  
18 hospital patient influx. To facilitate use of the model, we provide an R [5]  
19 [software package](#)<sup>5</sup> enabling anyone with access to similar data to develop  
20 a model tailored to specific patient and healthcare system characteristics  
21 and provide a [web-application](#)<sup>6</sup> that receives as input the characteristics of a  
22 patient and predicts the probabilities of different disease courses, including  
23 length-of-stay (LOS), probability of becoming critically ill, expected length-  
24 of-stay in critical state (LOSCS), and the probability of in-hospital mortality.  
25 Finally, we will share an anonymized version of the dataset used to develop  
26 the tool, where we shift hospitalization dates and aggregate age into 5-year  
27 categories.

## 28 **2. Methods**

29 We conducted a retrospective cohort study based on the Israeli Ministry of  
30 Health (MOH) COVID-19 hospitalized patient registry. The registry includes  
31 the patients' age and sex, dates and results of their severe acute respiratory  
32 syndrome corona virus-2 (SARS-COV-2) polymerase chain reaction (PCR)  
33 tests, dates of hospital admissions and discharge, *daily* clinical status dur-  
34 ing the admission (moderate, severe or critical, as detailed below), and the  
35 death registry. We included in the analyses all the patients who were ad-  
36 mitted between the 1st of March and the 2nd of May 2020 and who were  
37 hospitalized for at least 1 day. We excluded patients who were missing age  
38 or sex documentation. No data imputation was performed.

### 39 *2.1. Outcomes*

40 The primary outcome was predictions of the total and critical-care beds occu-  
41 pancy on a calendar scale which are due to the currently hospitalized patients  
42 and when the arrival process of new patients to the hospital at each day. We

---

<sup>5</sup><https://github.com/JonathanSomer/covid-19-multi-state-model>

<sup>6</sup><https://covid19-hospitalcourse.net/>

43 do this by predicting for each patient their day-by-day clinical state, includ-  
44 ing days in which the patient is in a critical state, non-critical, discharged,  
45 or possibly died. We further use the day-by-day clinical state predictions for  
46 predicting the overall risk for a single patient of being in a critical state at  
47 some point throughout hospitalization, risk of in-hospital mortality, expected  
48 hospital LOS and expected LOSCS.

## 49 2.2. Definitions

50 COVID-19 confirmed diagnosis was defined as a patient who was found to  
51 be positive for SARS-CoV-2 PCR tests [6]. Patients' clinical state during  
52 admission (mild or moderate, severe, and critical) was defined by the Is-  
53 raeli MOH guidelines, which are closely related to the National Institute for  
54 Health treatment guidelines [7]. A *mild* or *moderate* clinical state was de-  
55 fined as patients with symptoms such as fever, cough, sore throat, malaise,  
56 headache, or muscle pain, without shortness of breath, dyspnea on exertion,  
57 or abnormal imaging, or as patients with clinical or imaging evidence for  
58 lower respiratory disease and the saturation of oxygen ( $SpO_2$ )  $> 90\%$  on  
59 room air. For brevity we will refer to this state as *moderate* henceforth. A  
60 *severe* clinical state was defined as a patient with a respiratory rate higher  
61 than 30 breaths per minute,  $SpO_2 < 90\%$  on room air, or ratio of the arterial  
62 partial pressure of oxygen to fraction of inspired oxygen ( $PaO_2/FiO_2$ )  $< 300$   
63 mmHg. A *critical* clinical state was defined as a state where the patient suf-  
64 fers from respiratory failure which requires invasive/non-invasive mechanical  
65 ventilation, septic shock, or multiorgan dysfunction. In addition, we denote  
66 patients who were discharged from the hospital to their home or to out of  
67 hospital quarantine as *Discharged*. We note that discharged patients might  
68 be readmitted upon deterioration.

## 69 2.3. Statistical analysis methods

70 The clinical state of COVID-19 patients often alternates between moderate  
71 and more severe clinical states; see table S1 in supplementary materials (SM)  
72 for descriptive statistics of these transitions between clinical states. We mod-  
73 elled the way patients move between the different clinical states over time  
74 using a statistical machine learning approach. Specifically, we used an ap-  
75 proach whose purpose is exactly to model such processes: a multistate Cox  
76 regression-based survival analysis with right censoring, competing events, re-  
77 current events, left truncation, and time-dependent covariates, to model the  
78 way patients move between the different clinical states over time [8, 9, 10, 11].

79 The multistate model has 4 states: (1) moderate or severe, (2) critical, (3)  
80 discharged and (4) deceased. We chose to merge the moderate and severe  
81 clinical states due to sample size considerations. The model consists of six  
82 semiparametric Cox regression models, one for each possible state-to-state  
83 transition, as depicted in Figure 1; some transitions were excluded as either  
84 clinically implausible or due to few observed transitions. For details see SM  
85 sections 1.1 – 1.3.

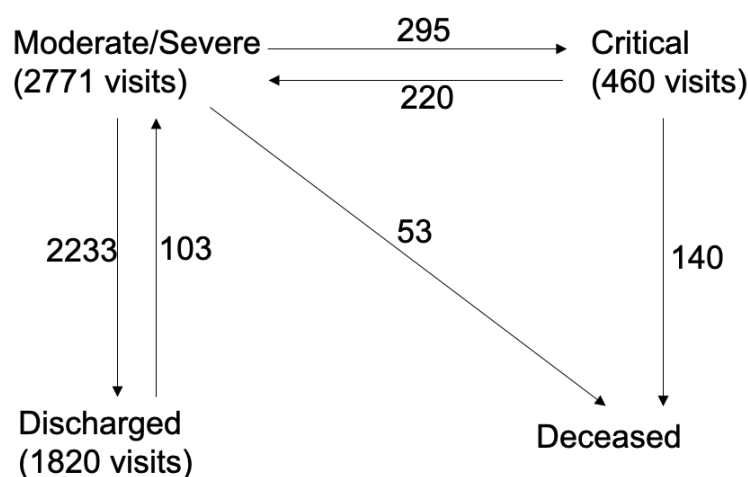


Figure 1: We model a COVID-19 patient’s disease course as moving between 4 possible states: (i) moderate or severe, (ii) critical, (iii) discharged and (iv) deceased. We combined the two clinical states moderate and severe into a single model state due to statistical considerations; however, we emphasize that we keep a distinction between the two by a covariate indicating whether the patient first entered at mild/moderate clinical state or at a severe clinical state. Numbers next to arrows indicate number of observed transitions; each patient can make several state transitions, and may visit a transient state more than once.

86 The six semiparametric models each took in age, sex, and state at hospi-  
87 talization as covariates; for the latter we kept the distinction between mod-  
88 erate and severe clinical states. We also added time-dependent covariates  
89 encoding the hospitalization history of the patient: cumulative days in hospi-  
90 tal, and whether the patient had been in a critical state before; see SM  
91 section 1.1.

92 Since hospitalization consists of potentially multiple transitions between  
93 transient states, the absolute risks, also known as the cumulative incidence

94 functions, do not have a tractable analytic form. Thus, we employed a  
95 method called Monte-Carlo (MC) sampling for obtaining unbiased estimates  
96 of patient and cohort statistics from the multistate model. Each MC sample  
97 for a given patient consists of a disease course (in terms of clinical states over  
98 time), conditioned on the patient’s history and covariates; this includes how  
99 long a patient spends in each clinical state. We calculated statistics such  
100 as median LOS or expected number of hospitalized patients per day based  
101 on aggregating the results of 20,000 MC samples for each patient. Standard  
102 errors were obtained by weighted bootstrap. See SM sections 1.4 and 1.7.

#### 103 *2.4. Model validation – hospital resource utilization and individual patient* 104 *disease course prediction*

105 We validated our model using 8-fold cross-validation – fitting the model on  
106 7/8 of the data and evaluating performance on the remaining held-out 1/8,  
107 repeated 8 times. Each held-out set consists of 330 patients.

108 We validated predictions of hospital utilization by two methods: “Snap-  
109 shot”, where we fix a set of patients and predict only this set’s utilization  
110 from a start date forward, without considering incoming patients, where the  
111 start date was chosen as either April 1st or April 15th 2020; and “Arrival  
112 process”, where we estimate utilization for the entire course of the first wave  
113 in Israel from March 1st to May 2nd 2020, over a held-out cohort of patients;  
114 see SM section 1.3 for description of both. For both validation methods we  
115 estimate the Mean Absolute Error (MAE) between the model’s predictions  
116 per-day and the actual number of hospitalized (or critical) patients on that  
117 day; the mean is over the number of days in the prediction window; see SM  
118 section 1.3.

119 We further validate the model’s performance by testing its predictions  
120 on the level of the individual patient: we use data from the first day of  
121 a patient’s admission to predict their probability of becoming critically ill  
122 (among patients who were non-critically ill on their 1st day) and the prob-  
123 ability of in-hospital mortality. For both outcomes we report Area Under  
124 Receiver Operating Characteristic (AUROC) with inverse weighting correc-  
125 tion for censoring, see SM section 1.3 for details. Finally, we validated the  
126 calibration of our predictions by tracking expected number of deaths vs. ac-  
127 tual number of deaths over time in an “Arrival+Snapshot” scenario, see SM  
128 section 1.3 for details.

129 *2.5. Using the model for prediction of hospital utilization under hypothetical*  
130 *scenarios*

131 In order to illustrate how our model may be employed for utilization predic-  
132 tion, we focus on a single held-out cohort of 330 patients. For this cohort  
133 we predict the total future hospital-bed and critical hospital-bed utilization  
134 up to 49 days ahead, starting from March 15th. Utilization for this cohort  
135 is composed of patients among the 330 who were hospitalized at the start-  
136 ing date and remain at the hospital, as well as utilization by newly arrived  
137 patients.

138 We present the expected hospital utilization and the number of deaths  
139 under three putative patient arrival scenarios (i) “younger”: rate and state  
140 of incoming patients are the same as in Israel during the weeks from March  
141 15th to May 2nd, but with patients in their 40s and 50s instead of 60+; (ii)  
142 “milder”: rate and age of incoming patients are the same as in Israel during  
143 the weeks from March 15th to May 2nd, but all patients incoming only in  
144 moderate or severe clinical state, none at critical, and (iii) “eldercare nursing  
145 home (NH) outbreak” where we assume that in addition to the arrival of  
146 patients as happened in Israel from March 15th to May 2nd there is a single  
147 week during which there are 4 times as many incoming patients aged 70+,  
148 arriving in various clinical states. The details of the scenarios are given in  
149 SM section 2.4.

150 **3. Results**

151 *3.1. Hospitalized patient characteristics*

152 The first patient with COVID-19 In Israel was diagnosed on February 27th  
153 2020. As of May 2nd 2020, 16,137 patients had confirmed positive diagnosis.  
154 The median (IQR) age of the confirmed patients was 33 (21-54); 44.5% were  
155 females. Out of the 16,137 confirmed COVID-19 patients up May 2nd, 2,703  
156 (17%) were hospitalized by May 2nd for at least one full day <sup>7</sup>. Of these  
157 2,703 hospitalized patients, 28 patients had no age or sex covariates. For the  
158 remaining cohort of 2,675 patients median (IQR) age was 58 (39-73), 44.19%  
159 were female. The demographics, medical history, and the clinical status of  
160 hospitalized patients are shown in Table 1. We use the model to estimate

---

<sup>7</sup>In addition, 30 patients were either dead on arrival or deceased within their first hospitalization day, and 5 were discharged on their first hospitalization day.

161 the median, 10% and 90% quantiles of the length-of-stay for hospitalized  
 162 patients stratified by clinical state at time of admission. The results are  
 163 shown in Figure 2 and Table S7 in the SM; in Table S8 in SM we report  
 164 LOSCS results.

LOS stratified by patients' age, sex and the clinical state at the time of admission

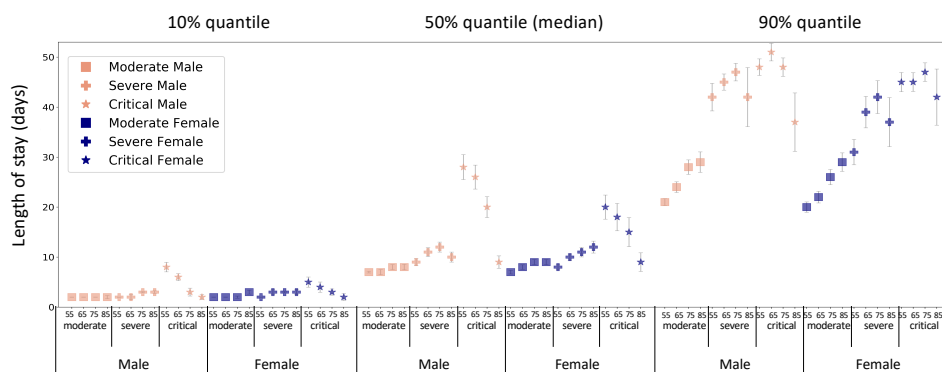


Figure 2: Model-based estimates of quantiles of length of stay in days based on 20,000 Monte Carlo results for each patient strata. Error bars indicate 95% confidence interval, calculated by weighted bootstrap.

165 In Table 2 we present the probability of different patient populations  
 166 entering a critical state and the probability for in-hospital mortality, as esti-  
 167 mated by the model. Both probabilities sharply increase with age; males of  
 168 all ages tend to have a greater probability of becoming critically ill compared  
 169 to females entering the hospital at the same clinical state, but hospitalized  
 170 Females over age 75 tend to have higher risk of mortality compared to hos-  
 171 pitalized males entering at comparable age and clinical state. Probabilities  
 172 and LOS and LOSCS quantiles for younger ages are given in Tables S5-S8  
 173 in the SM; for cumulative distribution function of LOS see Figure S2 in the  
 174 SM.

### 175 3.2. Cox models

176 The results for all six Cox models are given in Tables S2-S4 in the SM.

### 177 3.3. Model validation

178 The following results are all averaged over the 8 held-out validation cohorts.  
 179 Using “Snapshot” evaluation with April 1st as start data, MAE for pre-  
 180 dicting the per-day number of hospitalized patients is  $3.15 \pm 1.20$  for total



181 hospital-bed utilization and  $1.47 \pm 0.56$  for critical-care bed utilization. Using  
182 “Snapshot” evaluation with April 15th as start data, MAE for predicting the  
183 per-day number of hospitalized patients is  $3.13 \pm 1.07$  for total hospital-bed  
184 utilization and  $1.98 \pm 0.93$  for critical hospital-bed utilization. Using “Ar-  
185 rival” evaluation, MAE for predicting the per-day number of hospitalized  
186 patients is  $4.72 \pm 1.07$  for total hospital-bed utilization and  $1.68 \pm 0.40$  for  
187 critical hospital-bed utilization. See Table S9 and Figures S3-S4 in the SM  
188 for full results.

189 Using only information from the first day of a patient’s hospitalization,  
190 the AUROC for predicting in-hospital mortality and for predicting the out-  
191 come of becoming critically ill (among patients who were non-critically ill on  
192 their first day of admission) were  $0.96 \pm 0.04$  and  $0.88 \pm 0.04$  respectively; see  
193 Table S10 in the SM for full results. Table 3 presents the number of deaths  
194 predicted by our model under the true patient influx process (“Expected”  
195 column), which matches very closely the observed number of deaths, showing  
196 the model is well-calibrated.

### 197 *3.4. Predicting hospital-bed utilization*

198 In Figure 3 and Table 3 we show an example of the utilization and mortality  
199 projections generated by the model for several hypothetical scenarios.

200 As an example of how these scenarios could be useful for resource plan-  
201 ning, we consider the following use case for our model: COVID-19 patients  
202 are usually cared for in special wards. Our model can help planners assess  
203 when a new COVID-19 ward will need to open; towards that end, we add  
204 markers to Figure 3 indicating when total patient utilization passes multi-  
205 ples of 30, assuming that each COVID-19 ward can care for 30 patients. The  
206 intersection of the horizontal lines with the predicted utilization curve indi-  
207 cates at what date we estimate a new ward will need to be opened. Similarly,  
208 we add markers to show when critical patient utilization exceeds multiples  
209 of 15. In Figure S3 in the SM we show that the error for predicting the  
210 times when total hospital-bed utilization will hit such capacity thresholds is  
211 at most 1 day, and 3 days for critical-bed utilization.

## 212 **4. Discussion**

213 One of the distinctive characteristics of COVID-19 is the way health systems  
214 are overwhelmed by a large number of patients. For example, in Lombardy,  
215 Italy, ICU capacity reached its limit in early March, requiring urgent steps

216 and outside assistance [2]. Similar events occurred in Madrid [12], Wuhan  
217 [4], the city of New York [3], and other locations around the world.

218 We report here the development and validation of a multistate survival  
219 analysis model of patient clinical course throughout admission, discharge,  
220 and possibly death. Our model is based on the complete set of COVID-19  
221 patients in Israel, tracked day-by-day; we note we had a very small number  
222 of patients with missing data (28 out of 2703).

223 We show that using very simple and easily available patient character-  
224 istics, a machine learning methodology based on a set of Cox regression  
225 models can accurately predict healthcare utilization for a given patient ar-  
226 rival process and can be used to simulate utilization under different patient  
227 influx scenarios. This can in turn be used to accurately plan resource allo-  
228 cation and the opening or closing of COVID-19 wards. We further provide  
229 an anonymized version of the dataset used to develop the model, a [web-](#)  
230 [application](#) for patient level predictions, and an [R software package](#) that can  
231 help planners fit a multi-state model to their own data, or use the model we  
232 fit to the Israeli data.

233 Interestingly, we find that scenarios such as the arriving patients being  
234 much younger or in milder clinical state do not greatly affect total hospital  
235 utilization, possibly because some of these populations have longer hospi-  
236 talization times; on the other hand, both scenarios affect critical-care bed  
237 utilization. We further observe that an eldercare nursing home outbreak  
238 scenario leads to substantially higher total utilization and critical care uti-  
239 lization, underscoring the need to protect these communities not only in  
240 terms of preventing mortality, but also from the point of view of lowering the  
241 strain on hospital resources.

242 Many models exist for predicting the dynamics of COVID-19 case num-  
243 bers and numbers of hospitalized patients. These models are usually based  
244 on some variation of the basic susceptible-infected-recovered (SIR) model  
245 [13, 14], where the number of hospitalized patients are included as a compo-  
246 nent in the dynamic model.

247 Our model differs from these models in several aspects: (i) Settings in  
248 which the chance of experiencing one event is altered by the occurrence of  
249 other events are known as competing and semi-competing risks, and caution  
250 is needed in analyzing such data. In semi-competing risks a subject can  
251 experience both a nonterminal and terminal event where the terminal event  
252 (e.g., death) censors the nonterminal event (e.g. being in a critical state), but  
253 not vice-versa. Patient clinical course data consist of competing and semi-

254 competing risks. Ignoring (semi-) competing risks in time-to-event analyses  
255 can lead to substantially biased risk predictions [11, 15]. In this work we use  
256 a multi-state model as an excellent fit for the competing and semi-competing  
257 risks data of the COVID-19 patient hospitalization course. (ii) Heterogene-  
258 ity within and between patients is important, as bed utilization is in part  
259 determined by a long tail of some patients who require significantly longer  
260 stays than others. (iii) Our model has the capability of modeling patients on  
261 an individual basis and takes into account how long each patient has already  
262 been in the hospital. Thus, our model will take into account the case-mix and  
263 heterogeneous histories of the patients currently hospitalized when making  
264 predictions about future utilization. We also emphasize that our model is dif-  
265 ferent in its scope: we do not aim to model the spread of the disease and the  
266 number of future infections. Our focus is on estimating hospital-utilization  
267 under different patient arrival processes, while taking into account the load  
268 caused by currently hospitalized patients.

269 Another line of work related to ours are models for predicting outcomes  
270 for individual patients [16]. Viewed through this lens, our model is distinctive  
271 in two ways: it provides time-to-event (release, deterioration, death) predic-  
272 tions, and it is based on a very small number of covariates (age, sex, and one  
273 of three patient clinical states). For example, Liang et al. [17] report AUROC  
274 of 0.88 for predicting critical illness or death using 10 covariates selected from  
275 72 potential predictors. Bello-Chavolla et al. [18] report a concordance of 0.83  
276 using 7 covariates based mostly on comorbidities. We conjecture that the ac-  
277 curacy achieved by our model while using minimal, easily obtainable data as  
278 input might be explained by the fact that patients' clinical states are at least  
279 partially a mirror for more granular clinical measures and comorbidities not  
280 available to us.

281 Our model has several limitations. First, it is based on data from the  
282 first wave of patients in Israel. As treatment strategies and hospitalization  
283 policies differ over time and between health systems and hospitals, we can-  
284 not guarantee that LOS statistics will be the same across all locales and  
285 times. Thus, when possible we encourage planners to use the attached [soft-  
286 ware package](#) and fit it to their own hospitalization data. We will update  
287 the software package and app as more updated data will become available  
288 from the Israeli registry. A second limitation is that our model must rely  
289 on predictions for who will the incoming patients be. If arriving patient  
290 populations – both patient type and patient numbers – will differ signifi-  
291 cantly from the scenarios taken into account, the model's predictions will be

292 wrong. We thus recommend that planners evaluate multiple hypotheticals  
293 for incoming patients, testing for scenarios such as the ones we presented in  
294 the Results section above. A third limitation is that the model does not take  
295 into account patients' comorbidities [19, 20, 21]. On the one hand, our model  
296 achieves good results while analyzing only a limited number of covariates as  
297 input; on the other hand, it is possible that using comorbidities could en-  
298 hance the model's performance. We also wish to point out that researchers  
299 with access to patient-level comorbidity data can easily incorporate it into a  
300 multistate model using the software we provide. A fourth limitation is that  
301 we used the patients' clinical state as reported by the attending physician at  
302 the point of care. Although the Israeli MOH directed physicians to report  
303 clinical state using the definitions above, individual physicians and medical  
304 centers might not have adhered exactly to these guidelines. We note that  
305 despite this possible ambiguity, empirically we find that the clinical state as  
306 reported is indeed predictive for individual patients.

## 307 **5. Conclusions**

308 We found that a very small set of covariates (age, sex and patient being in  
309 one of three clinical states), along with a day-by-day tracking of patients'  
310 clinical state, are enough for accurate predictions of mortality, length-of-  
311 hospitalization and critical illness. These accurate predictions enable us to  
312 build a tool that lets healthcare managers accurately plan resource allocation  
313 for COVID-19 patient care in the face of potentially large patient surges.

## 314 **6. Acknowledgments**

315 We thank Dr. Amit Huppert and the biostatistics unit researchers at Gertner  
316 Institute for their insights and help in conducting this study. We thank Prof.  
317 Orly Manor for her valuable comments on the manuscript. We further wish to  
318 thank the Medical division and Information and Technologies division of the  
319 Israeli Ministry of Health for their efforts in the gathering and organization  
320 of the clinical data from all the Israeli hospitals. We thank the information  
321 and technologies staff of medical centers across Israel for building the data  
322 infrastructure needed for the collection of the data used in this study.

---

<sup>8</sup>Patients who were hospitalized for at least 1 full day. Excluded are 28 patients for which we had missing age or sex information.

Table 1: Demographics and clinical characteristics of patients in the Israeli COVID-19 registry who were Hospitalized between March 1st and May 2nd.

Characteristic	Total, mean (SD) [range]	Critical by May 2nd	In-hospital mortality by May 2nd	Still hospitalized on May 2nd
<b>No.</b>	2,675 <sup>8</sup> (100%)	437 (16.34%)	200 (7.48%)	311 (11.63%)
<b>Female, No. (%)</b>	1,171 (43.78%)	146 (33.41%)	89 (44.5%)	130 (42%)
<b>Age, mean (SD) y</b>	55.3 (21.7)	71 (16.35)	80.66 (12.78)	65.5 (20.01)
<b>Age, No. (%):</b>				
< 20	106 (3.96%)	3 (0.69%)	0 (0%)	8 (2.57%)
20-29	316 (11.81%)	4 (0.92%)	0 (0%)	15 (4.82%)
30-39	272 (10.17%)	14 (3.2%)	2 (1%)	20 (6.43%)
40-49	330 (12.34%)	19 (4.35%)	3 (1.5%)	15 (4.82%)
50-59	401 (15%)	57 (13.04%)	6 (3%)	36 (11.58%)
60-69	458 (17.12%)	79 (18.08%)	20 (10%)	56 (18%)
70-79	412 (15.4%)	118 (27%)	50 (25%)	80 (25.72%)
80+	380 (14.21%)	143 (32.72%)	119 (59.5%)	81 (26.05%)
<b>Initial state:</b>				
Moderate	2048 (76.56%)	113 (25.8%)	50 (25%)	164 (52.73%)
Severe	432 (16.14%)	129 (29.5%)	66 (33%)	83 (26.69%)
Critical	195 (7.29%)	195 (44.6%)	84 (42%)	64 (20.58%)

## 323 References

- 324 [1] World Health Organization, Situation report - 18 situation  
325 in numbers total and new cases in last 24 hours, [https://www.who.int/docs/default-source/coronaviruse/situation-reports/](https://www.who.int/docs/default-source/coronaviruse/situation-reports/20200311-sitrep-51-covid-19.pdf?sfvrsn=1ba62e57_10)  
326 [20200311-sitrep-51-covid-19.pdf?sfvrsn=1ba62e57\\_10](https://www.who.int/docs/default-source/coronaviruse/situation-reports/20200311-sitrep-51-covid-19.pdf?sfvrsn=1ba62e57_10), 2020. Accessed:  
327 May 10th, 2020.  
328

<sup>9</sup>Probabilities are based on Monte Carlo results, with weighted bootstrap 95% confidence interval.

Table 2: Probability of death and probability of becoming critical by patient type (state at time of hospitalization, age, sex).

<i>Incoming state, age</i>	Probability of in-hospital mortality		Probability of becoming critical	
	<i>Male</i>	<i>Female</i>	<i>Male</i>	<i>Female</i>
Moderate, 55	0.9% <sup>9</sup> (0.2%, 1.5%)	1.3% (0.4%, 2.3%)	5.9% (4.6%, 7.3%)	4.1% (2.5%,5.7%)
Moderate, 65	2.2% (1.2%, 3.2%)	2.6% (1.2%, 4%)	8.5% (6.9%, 10.1%)	6.1% (4.1%,8%)
Moderate, 75	5.8% (3.4%, 7.8%)	5.3% (3%, 7.6%)	12.9% (10.5%, 15.2%)	9.9% (6.9%,12.8%)
Moderate, 85	15.1% (8.9%, 21.2%)	12.2% (7.6%, 16.7%)	17.9% (13.9%, 21.9%)	13.4% (8.9%,17.9%)
Severe, 55	4.3% (0%, 9.5%)	7.5% (1.2%, 13.7%)	24.1% (18.7%, 29.4%)	18.5% (12.8%,24.2%)
Severe, 65	9.6% (3.9%, 15.2%)	12.6% (4.3%, 20.8%)	31.9% (26.7%, 37.0%)	25.6% (20.1%,31.1%)
Severe, 75	21.4% (14.9%,28%)	21.7% (12.6%,30.9%)	40.4% (35%, 45.7%)	32.3% (26.7%,37.9%)
Severe, 85	44.3% (32.3%,56.3%)	38.9% (28.8%,48.9%)	46.7% (39.3%, 56.3%)	38.5% (31.1%,45.8%)
Critical, 55	15.3% (3.5%, 27.2%)	29.9% (10.8%, 49%)	100%	100%
Critical, 65	29.9% (17.9%,41.9%)	41.4% (25.5%,57.2%)	100%	100%
Critical, 75	54.6% (42.9%,66.3%)	54.9% (42.6%,67.1%)	100%	100%
Critical, 85	82.9% (74.4%,91.3%)	75.4% (65.2%,85.7%)	100%	100%

Table 3: Number of deaths (in-hospital mortality) within a random subset of 330 validation set (held-out) patients. “Observed” is true number of deaths, “Expected” is prediction by the model. “Younger”, “Milder” and “NH Outbreak” are hypothetical scenarios, see Methods above.

Days	Observed	Expected	<i>Hypothetical scenarios</i>		
			Younger	Milder	NH Outbreak
5	7	6.5	0.6	3.7	8.2
10	16	16.6	1.9	11.7	22.6
15	20	20.4	2.5	15	28.3
20	23	22.8	3	17.3	32.1
25	24	25.4	3.4	19.7	36.5
30	25	25.9	3.5	20.1	37
35	26	26.6	3.7	20.6	37.7

- 329 [2] G. Grasselli, A. Pesenti, M. Cecconi, Critical care utilization for the  
330 COVID-19 outbreak in Lombardy, Italy: early experience and forecast  
331 during an emergency response, *Jama* 323 (2020) 1545–1546.
- 332 [3] A. W. Peters, K. S. Chawla, Z. A. Turnbull, Transforming ORs into  
333 ICUs, *New England Journal of Medicine* 382 (2020) e52.
- 334 [4] R. Li, C. Rivers, Q. Tan, M. B. Murray, E. Toner, M. Lipsitch, Esti-  
335 mated demand for US hospital inpatient and intensive care unit beds  
336 for patients with COVID-19 based on comparisons with Wuhan and  
337 Guangzhou, china, *JAMA network open* 3 (2020) e208297–e208297.
- 338 [5] R Core Team, R: A Language and Environment for Statistical Com-  
339 puting, R Foundation for Statistical Computing, Vienna, Austria, 2017.  
340 URL: <https://www.R-project.org/>.
- 341 [6] Centers for Disease Control and Prevention, ICD-10-CM official coding  
342 and reporting guidelines April 1, 2020 through September 30, 2020, 2020.
- 343 [7] National Institutes of Health, Management of COVID-19 — coro-  
344 navirus disease COVID-19, [https://www.covid19treatmentguidelines.  
345 nih.gov/overview/management-of-covid-19/](https://www.covid19treatmentguidelines.nih.gov/overview/management-of-covid-19/), 2020. Accessed August 16,  
346 2020.

- 347 [8] P. K. Andersen, R. D. Gill, Cox's regression model for counting pro-  
348 cesses: a large sample study, *The annals of statistics* (1982) 1100–1120.
- 349 [9] P. K. Andersen, L. S. Hansen, N. Keiding, Non-and semi-parametric  
350 estimation of transition probabilities from censored observation of a non-  
351 homogeneous markov process, *Scandinavian Journal of Statistics* (1991)  
352 153–167.
- 353 [10] J. P. Klein, M. L. Moeschberger, *Survival analysis: techniques for cen-  
354 sored and truncated data*, Springer Science & Business Media, 2006.
- 355 [11] J. D. Kalbfleisch, R. L. Prentice, *The statistical analysis of failure time  
356 data*, volume 360, John Wiley & Sons, 2011.
- 357 [12] E. Condes, J. R. Arribas, et al., Impact of COVID-19 on Madrid hospital  
358 system, *Enfermedades Infecciosas Y Microbiologia Clinica* (2020).
- 359 [13] G. E. Weissman, A. Crane-Droesch, C. Chivers, T. Luong, A. Hanish,  
360 M. Z. Levy, J. Lubken, M. Becker, M. E. Draugelis, G. L. Anesi, et al.,  
361 Locally informed simulation to predict hospital capacity needs during  
362 the COVID-19 pandemic, *Annals of internal medicine* (2020).
- 363 [14] S. M. Moghadas, A. Shoukat, M. C. Fitzpatrick, C. R. Wells, P. Sah,  
364 A. Pandey, J. D. Sachs, Z. Wang, L. A. Meyers, B. H. Singer, et al.,  
365 Projecting hospital utilization during the COVID-19 outbreaks in the  
366 United States, *Proceedings of the National Academy of Sciences* 117  
367 (2020) 9122–9126.
- 368 [15] A. Oulhaj, L. A. Ahmed, J. Prattes, A. Suliman, A. Al Suwaidi, R. H.  
369 Al-Rifai, H. Sourij, I. Van Keilegom, The competing risk between in-  
370 hospital mortality and recovery: A pitfall in COVID-19 survival analysis  
371 research, *medRxiv* (2020).
- 372 [16] L. Wynants, B. Van Calster, M. M. Bonten, G. S. Collins, T. P. Debray,  
373 M. De Vos, M. C. Haller, G. Heinze, K. G. Moons, R. D. Riley, et al.,  
374 Prediction models for diagnosis and prognosis of COVID-19 infection:  
375 systematic review and critical appraisal, *BMJ* 369 (2020).
- 376 [17] W. Liang, H. Liang, L. Ou, B. Chen, A. Chen, C. Li, Y. Li, W. Guan,  
377 L. Sang, J. Lu, et al., Development and validation of a clinical risk score



- 378 to predict the occurrence of critical illness in hospitalized patients with  
379 COVID-19, *JAMA Internal Medicine* (2020).
- 380 [18] O. Y. Bello-Chavolla, J. P. Bahena-López, N. E. Antonio-Villa,  
381 A. Vargas-Vázquez, A. González-Díaz, A. Márquez-Salinas, C. A.  
382 Fermín-Martínez, J. J. Naveja, C. A. Aguilar-Salinas, Predicting mor-  
383 tality due to SARS-CoV-2: A mechanistic score relating obesity and  
384 diabetes to COVID-19 outcomes in Mexico, *The Journal of Clinical*  
385 *Endocrinology & Metabolism* 105 (2020).
- 386 [19] J. L. Atkins, J. A. Masoli, J. Delgado, L. C. Pilling, C.-L. Kuo, G. A.  
387 Kuchel, D. Melzer, Preexisting comorbidities predicting COVID-19 and  
388 mortality in the UK Biobank community cohort, *The Journals of Geron-*  
389 *tology: Series A* (2020).
- 390 [20] C. M. Petrilli, S. A. Jones, J. Yang, H. Rajagopalan, L. O'Donnell,  
391 Y. Chernyak, K. A. Tobin, R. J. Cerfolio, F. Francois, L. I. Horwitz,  
392 Factors associated with hospital admission and critical illness among  
393 5279 people with coronavirus disease 2019 in New York City: prospec-  
394 tive cohort study, *BMJ* 369 (2020).
- 395 [21] L. Fang, G. Karakiulakis, M. Roth, Are patients with hypertension and  
396 diabetes mellitus at increased risk for COVID-19 infection?, *The Lancet.*  
397 *Respiratory Medicine* 8 (2020) e21.

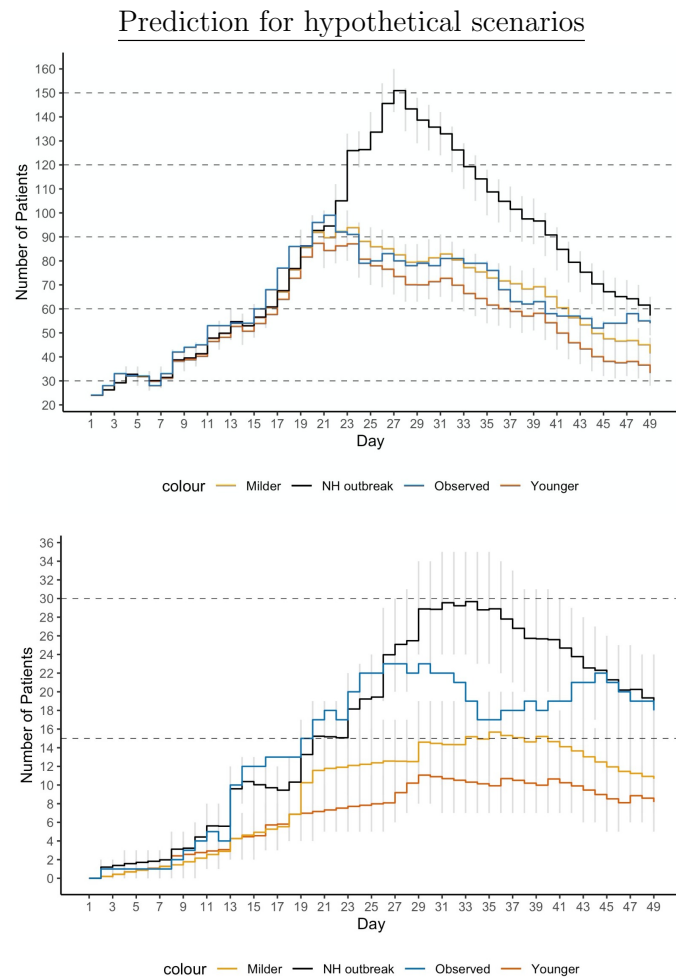


Figure 3: Observed total hospitalized (top) and critical (bottom) patients, and predicted total number of hospitalized patients. under the following scenarios (i) “younger”: rate and state of incoming patients are the same as in Israel during the weeks from March 15th to May 2nd, but with patients in their 50s and 60s instead of 60+; (ii) “milder”: rate and age of incoming patients are the same as in Israel during the weeks from March 15th to May 2nd, but all patients incoming only in moderate and severe state, none at critical, and (iii) “Nursing home (NH) outbreak” where we assume that in addition to the arrival of patients as happened in Israel from March 15th to May 2nd there is a single week during which there are 4 times as many incoming patients aged 70+, arriving in various clinical states. Gray vertical lines are point-wise 10%-90% confidence predictions.

## Supplementary Material

## Contents

<b>1</b>	<b>Models and Methods</b>	<b>3</b>
1.1	Introduction . . . . .	3
1.2	Estimation . . . . .	4
1.3	Predictions . . . . .	6
1.4	Monte Carlo Estimator of Length of Stay . . . . .	7
1.5	Path Sampling - Technical Details . . . . .	8
1.6	Predictions at the Patient Level - Technical Details . . . . .	10
1.7	Weighted Bootstrap Standard Error for Prediction at the Subject Level . . . . .	12
1.8	Prediction at the Health-System Level . . . . .	12
<b>2</b>	<b>Results</b>	<b>13</b>
2.1	Prediction at the Patient Level . . . . .	13
2.2	Prediction at the Health System Level - Random Subset of Patients 8-fold Cross Validation . . . . .	14
2.3	Prediction at the Health System Level - Hospital Holdout . . . . .	14
2.4	Prediction at the Health System Level - Hypothetical Scenarios . . . . .	15

# 1 Models and Methods

## 1.1 Introduction

The hospitalization course of each patient is described as a multi-state process, depicted in Figure S1. A patient enters the hospital at one of the following three clinical states: moderate, severe or critical. During the course of hospitalization a patient can move among the transient clinical states: Critical, denoted by  $C$ ; Moderate or Severe, denoted by  $M/S$ ; and Discharged, denoted by  $Di$ . Our multi-state model combines Moderate and Severe, during hospitalization, due to the small number of observed transitions from and to each of these states, separately. The state  $Di$  is considered as a transient state rather than a terminal state since frequently patients in a milder state were released from hospital to a dedicated quarantine for COVID-19 patients, with some later experiencing deterioration leading to re-hospitalization; in Figure S1 we see there were 102 transitions from state  $Di$  to state  $M/S$ . The terminal state Deceased is denoted by  $De$ .

Our multi-state model allows the following six transitions

$$C \rightarrow M/S \quad C \rightarrow De \quad M/S \rightarrow De \quad M/S \rightarrow C \quad M/S \rightarrow Di \quad Di \rightarrow M/S.$$

Three transitions were excluded from the model due to small sample size: The dataset includes 10 records of transition  $C \rightarrow Di$ , no records of  $Di \rightarrow De$ , and 2 records of  $Di \rightarrow C$ . Hence, these three transitions were excluded from the multi-state model. Each possible transition is characterized by a transition-specific Cox proportional hazard model with an unspecified transition-specific baseline hazard function,  $\lambda_{0,\cdot}$ , and a transition-specific vector  $\beta_{\cdot}$ , of regression coefficients. Specifically, for  $t > 0$ , the corresponding Cox proportional hazard functions are

$$\lambda_{C,M/S}(t|Z) = \lambda_{0C,M/S}(t) \exp(\beta_{C,M/S}^T Z), \quad (1)$$

$$\lambda_{C,De}(t|Z) = \lambda_{0C,De}(t) \exp(\beta_{C,De}^T Z), \quad (2)$$

$$\lambda_{M/S,Di}(t|Z) = \lambda_{0M/S,Di}(t) \exp(\beta_{M/S,Di}^T Z), \quad (3)$$

$$\lambda_{M/S,C}(t|Z) = \lambda_{0M/S,C}(t) \exp(\beta_{M/S,C}^T Z), \quad (4)$$

$$\lambda_{M/S,De}(t|Z) = \lambda_{0M/S,De}(t) \exp(\beta_{M/S,De}^T Z), \quad (5)$$

and

$$\lambda_{Di,M/S}(t|Z) = \lambda_{0Di,M/S}(t) \exp(\beta_{Di,M/S}^T Z), \quad (6)$$

where  $Z$  is a vector of covariates, possibly with time-dependent covariates. For simplicity of notation, we use  $Z$  instead of  $Z(t)$  whenever confusion is unexpected. Although  $Z$  is shared by the six models above, it does not imply that identical covariates must be used in these models, since the regression coefficient vectors,  $\beta_{\cdot,\cdot}$ , are transition dependent, and one can set any specific coefficient to 0 in order to exclude the corresponding covariate.

The covariates included in the Cox models were: age, sex, state at time of hospitalization (three categories: Moderate, Severe, or Critical), a binary variable equal to 1 if the patient previously was in a critical state and 0 otherwise, the cumulative number of days in hospital at entry time to the current state, and the interaction between age and each of the other covariates listed above. The models of transitions  $M/S \rightarrow De$  and  $Di \rightarrow M/S$  are slightly different due to only a few events with a critical clinical state at time of hospital admission and a few events with previous visits in critical state. Therefore, for these two models, the binary covariate taking the value of 1 if the patient previously visited the critical state is excluded, and the covariate for clinical state at time of hospitalization was redefined as a binary covariate indicating Moderate versus Severe/Critical.

## 1.2 Estimation

Estimating the above hazard functions (1)–(6) involves several major issues (beside right censoring), which we describe below: multi-state process, left truncation, competing risks and recurrent events.

**Multi-state process:** We describe the hospitalization path of each patient as a multi-state process, starting at states  $C$  or  $M/S$ . Each patient may visit a transient state ( $C$ ,  $M/S$  or  $Di$ ) multiple times before reaching a terminal state ( $De$ ).

**Left truncation:** Consider, for example, a patient who entered the hospital at state  $M/S$  and moved to state  $C$  at the 10th day of hospitalization. The contribution of such a patient to transitions from state  $C$  (back to  $M/S$  or to  $De$ ) starts only at the 10th day of hospitalization. Hence, when estimating the model of a certain transition from origin state

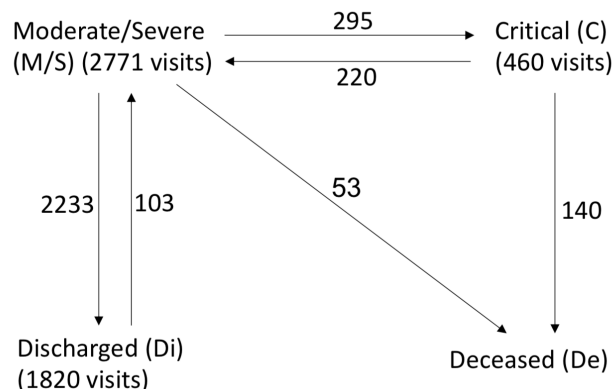


Figure S1: Multi-State Model: Data as of May 2, 2020,  $n = 2675$ . We model a COVID-19 patients disease course as moving between 4 possible clinical states: (i) moderate or severe, (ii) critical, (iii) discharged and (iv) deceased. We combined the two clinical states moderate and severe into a single model state due to statistical considerations; however, we keep a distinction between the two by a covariate indicating whether the patient first entered at mild/moderate clinical state or at a severe clinical state. Numbers next to arrows indicate number of observed transitions; each patient can make several clinical state transitions, and may visit a transient clinical state more than once. The dataset includes 10 records of transitions  $C \rightarrow Di$ , no records of  $Di \rightarrow De$ , and 2 records of  $Di \rightarrow C$ . Hence, these three transitions were excluded from the multi-state model.

(e.g.  $C$ ) to a target state (e.g.  $De$ ), those who entered the origin state during the course of hospitalization are left-truncated by their entering day to that origin state.

**Competing risks (competing events):** Given that a patient is, for example, at state  $C$ , there are two possible transitions:  $C \rightarrow M/S$  and  $C \rightarrow De$ . Since only one of these transitions can occur at each point in time,  $M/S$  and  $De$  are competing events in the sense that at each time point, the occurrence of one type of event will prevent the occurrence of the other. Similarly, given that a patient is at state  $M/S$ , the events  $Di$ ,  $C$  and  $De$  are competing events.

**Recurrent events:** A patient may visit states  $C$ ,  $M/S$  and  $Di$  multiple times. For example, 13 patients had the following hospitalization path

$$M/S \rightarrow C \rightarrow M/S \rightarrow C \rightarrow M/S \rightarrow Di,$$

and 68 patients had

$$M \rightarrow Di \rightarrow M/S \rightarrow Di.$$

All the observed paths and their frequencies are provided in Table S1. When the event of interest can occur more than once in a patient, the events are termed recurrent events.

We overcame all the above challenges and provided consistent estimators (under mild regularity conditions) for the six Cox proportional hazard models. Specifically, by extending the approach of Andersen et al. (1991), it can be shown that maximizing the likelihood function in terms of the six Cox models can be done by maximizing the likelihood of each transition separately, while using the risk-set correction for dealing with left truncation (Klein & Moeschberger, 2006); treating competing transitions as right censoring (Kalbfleisch & Prentice, 2011); and adopting Andersen-Gill approach for dealing with recurrent events so the robust standard errors account for correlated outcomes within a patient (Andersen & Gill, 1982).

### 1.3 Predictions

Based on our multi-state model, we accurately predict at the **patient level**, given age, sex and state at time of hospitalization, the following quantities:

1. The chance of in-hospital mortality (state  $De$ ).
2. The chance of being at a critical state (state  $C$ ).
3. The total length of stay (LOS) in hospital (not including time in a dedicated out-of-hospital quarantine).
4. The total length of stay in critical state (LOSCS).

The above quantities can be predicted at the first day of hospitalization and also during the course of hospitalization, while correctly taking into account the accumulated hospitalization history.

Weighted estimators of the area under the Receiver Operating Characteristic curve (AUROC) were used to evaluate death and critical-visit predictions for binary classifications (i.e. yes/no in-hospital mortality and yes/no previously visiting critical state). The



weights eliminate the bias due to exclusion of censored observations, and were defined as 1 over the probability of being uncensored (Robins & Finkelstein, 2000). The weights were estimated by a Kaplan-Meier estimator of the censoring survival function. Weighted AU-ROC estimates were calculated by the R package WeightedROC (Hocking, 2020). Brier scores were used as measures of prediction accuracy.

Based on the above predictions, we go one step further and provide predictions at the **hospital level**, in the following manner:

1. **Snapshot:** Assume that at a given calendar day, we are given the current state and hospitalization history of all the COVID-19 patients currently at a specific hospital. Beyond predicting the above quantities for each patient, we also predict the total number of patients at the hospital, and at a critical clinical state in particular, for each day over the next 8 weeks. Namely, we provide predictions on the total occupancy on a calendar scale which are only due to the currently hospitalized patients.
2. **Arrival:** Given as input the arrival process of patients to the hospital at each day, including the number of arriving patients, their age, sex and state at time of hospitalization, we predict the total number of patients at hospital, and at critical state in particular, for each day of the next 8 weeks. Here we provide a prediction for the total occupancy on a calendar scale, for any possible hypothetical arrival scenario.
3. **Arrival plus Snapshot:** At a given calendar day, we are given the current state and hospitalization history of all the COVID-19 patients currently at the hospital along with an arrival process of the patients to be hospitalized starting the next day up to a pre-specified time period. Again, we predict the total number of patients at hospital, and at critical state in particular, on a calendar scale.

## 1.4 Monte Carlo Estimator of Length of Stay

Since our hospitalization model consists of a multi-state model with recurring events (i.e. a patient can visit a transient state multiple times) the closed form marginal probabilities required for predictions are intractable. Instead we use a Monte Carlo (MC) approach for estimating all the required quantities listed above (Section 1.3).

Assume a prediction is desired for a new patient with baseline covariates (i.e. age, sex, and clinical state at time of hospitalization) denoted by  $X$ . The MC-based prediction procedure can be summarized as follows. Given  $X$ , sample a large number (e.g. 20,000) of hospitalization paths, and use these paths for estimating the required quantities. Specifically, the probability of death is estimated by the proportion of paths ended at state  $De$ ; the probability of visiting state  $C$  is estimated by the proportion of paths visited state  $C$ ; the expected total length of stay is estimated by the mean length of the paths (not including time at state  $Di$ ); and the expected length of stay in state  $C$  is estimated by the mean time spent in state  $C$  over all the paths. The next subsection provides a detailed description of path sampling.

## 1.5 Path Sampling - Technical Details

Let  $J_C$  and  $J_N$  denote the current and next states, respectively. Assume a patient entered the hospital at state  $J_C = j^*$  with a vector of baseline covariates  $X$ . The goal is to provide a MC estimator of the length of hospitalization given  $X$  and  $j^*$ . Let  $Z(t)$  be a time-dependent vector of covariates such that  $Z(t) = (X^T, \tilde{X}(t)^T)^T$ , where  $\tilde{X}(t)$  is a time-dependent vector of covariates that are known at the entrance to the new state. Details of  $\tilde{X}(t)$  in our setting are provided at the end of Section 1.1. Assume  $K_{j^*}$  possible transitions from state  $j^*$ . For each state  $j$ ,  $j = 1, \dots, K_{j^*}$ ,

$$\begin{aligned} & \Pr(T \leq t, J_N = j | J_C = j^*, Z(0) = Z) \\ &= \int_0^t \exp(\beta_{j^*,j}^T Z) \lambda_{0j^*,j}(u) \exp \left\{ - \sum_{k=1}^{K_{j^*}} \Lambda_{0j^*,k}(u) \exp(\beta_{j^*,k}^T Z) \right\} du, \end{aligned}$$

where  $\beta_{j^*,j}$ ,  $\lambda_{0j^*,j}$  and  $\Lambda_{0j^*,j}$  are the vector of regression coefficients, the baseline hazard function and the cumulative baseline hazard function of transition  $j^* \rightarrow j$ , respectively.

Then,

$$\begin{aligned} & \Pr(J_N = j | J_C = j^*, Z(0) = Z) \\ &= \int_0^\infty \exp(\beta_{j^*,j}^T Z) \lambda_{0j^*,j}(u) \exp \left\{ - \sum_{k=1}^{K_{j^*}} \Lambda_{0j^*,k}(u) \exp(\beta_{j^*,k}^T Z) \right\} du \end{aligned}$$

and

$$\begin{aligned} & \Pr(T \leq t | J_N = j, J_C = j^*, Z(0) = Z) \\ &= \frac{\int_0^t \exp(\beta_{j^*,j}^T Z) \lambda_{0j^*,j}(u) \exp \left\{ - \sum_{k=1}^{K_{j^*}} \Lambda_{0j^*,k}(u) \exp(\beta_{j^*,k}^T Z) \right\} du}{\int_0^\infty \exp(\beta_{j^*,j}^T Z) \lambda_{0j^*,j}(u) \exp \left\{ - \sum_{k=1}^{K_{j^*}} \Lambda_{0j^*,k}(u) \exp(\beta_{j^*,k}^T Z) \right\} du}. \end{aligned}$$

We start by describing the sampling procedure of the next state. Let  $\tau_{j^*,j}$  be the largest observed event time of transition  $j^* \rightarrow j$ . Then, the next state is sampled from a  $K_{j^*}$  multinomial distribution with probabilities  $p_{j|j^*,Z}$  where, for  $j = 1, \dots, K_{j^*}$ ,

$$\begin{aligned} & \widehat{\Pr}(J_N = j | J_C = j^*, Z(0) = Z) \\ &= \sum_{t_m \leq \tau_{j^*,j}} \exp(\widehat{\beta}_{j^*,j}^T Z) \widehat{\lambda}_{0j^*,j}(t_m) \exp \left\{ - \sum_{k=1}^{K_{j^*}} \widehat{\Lambda}_{0j^*,k}(t_{m-1}) \exp(\widehat{\beta}_{j^*,k}^T Z) \right\}, \end{aligned}$$

the summation is over the distinct observed event times of transition  $j^* \rightarrow j$  and

$$p_{j|j^*,Z} = \frac{\widehat{\Pr}(J_N = j | J_C = j^*, Z(0) = Z)}{\sum_{j'=1}^{K_{j^*}} \widehat{\Pr}(J_N = j' | J_C = j^*, Z(0) = Z)}. \quad (7)$$

Once we sampled the next state, denoted by  $j'$ , the time to be spent at state  $j^*$  should be sampled based on

$$\begin{aligned} & \widehat{\Pr}(T \leq t | J_N = j', J_C = j^*, Z(0) = Z) \\ &= \frac{\sum_{t_m \leq t} \exp(\widehat{\beta}_{j^*,j'}^T Z) \widehat{\lambda}_{0j^*,j'}(t_m) \exp \left\{ - \sum_{k=1}^{K_{j^*}} \widehat{\Lambda}_{0j^*,k}(t_{m-1}) \exp(\widehat{\beta}_{j^*,k}^T Z) \right\}}{\sum_{t_m \leq \tau_{j^*,j'}} \exp(\widehat{\beta}_{j^*,j'}^T Z) \widehat{\lambda}_{0j^*,j'}(t_m) \exp \left\{ - \sum_{k=1}^{K_{j^*}} \widehat{\Lambda}_{0j^*,k}(t_{m-1}) \exp(\widehat{\beta}_{j^*,k}^T Z) \right\}}. \quad (8) \end{aligned}$$

This could be done by sampling  $U \sim Uniform[0, 1]$ , equating

$$U = \widehat{\Pr}(T \leq t | J_N = j', J_C = j^*, Z(0) = Z)$$

and solving for  $t$ . Denote the sampled time by  $t'$  and update  $Z(t')$ . In case  $j' = De$ , the sampling path ends here. Otherwise, the current state is updated to  $J_C = j'$ , and the following state is sampled by  $p_{j|j',Z}$ , where for  $j = 1, \dots, K_{j'}$

$$p_{j|j',Z} = \frac{\sum_{t' < t_m \leq \tau_{j',j}} \exp\left(\widehat{\beta}_{j',j}^T Z\right) \widehat{\lambda}_{0j',j}(t_m) \exp\left\{-\sum_{k=1}^{K_{j'}} \widehat{\Lambda}_{0j',k}(t_{m-1}) \exp\left(\widehat{\beta}_{j',k}^T Z\right)\right\}}{\sum_{j^{**}=1}^{K_{j'}} \sum_{t' < t_m \leq \tau_{j',j^{**}}} \exp\left(\widehat{\beta}_{j',j^{**}}^T Z\right) \widehat{\lambda}_{0j',j^{**}}(t_m) \exp\left\{-\sum_{k=1}^{K_{j'}} \widehat{\Lambda}_{0j',k}(t_{m-1}) \exp\left(\widehat{\beta}_{j',k}^T Z\right)\right\}} \quad (9)$$

An exceptional state is  $J_C = Di$ , where one can either move back to  $M/S$  or stay at  $Di$ .

Given the new sampled state, denoted by  $\check{j}$ , the time to be spent at  $j'$  is sampled by

$$\begin{aligned} & \widehat{\Pr}(T \leq t | J_N = \check{j}, J_C = j', Z(t') = Z) \\ &= \frac{\sum_{t' < t_m \leq t} \exp\left(\widehat{\beta}_{j',\check{j}}^T Z\right) \widehat{\lambda}_{0j',\check{j}}(t_m) \exp\left\{-\sum_{k=1}^{K_{j'}} \widehat{\Lambda}_{0j',k}(t_{m-1}) \exp\left(\widehat{\beta}_{j',k}^T Z\right)\right\}}{\sum_{t' < t_m \leq \tau_{j',\check{j}}} \exp\left(\widehat{\beta}_{j',\check{j}}^T Z\right) \widehat{\lambda}_{0j',\check{j}}(t_m) \exp\left\{-\sum_{k=1}^{K_{j'}} \widehat{\Lambda}_{0j',k}(t_{m-1}) \exp\left(\widehat{\beta}_{j',k}^T Z\right)\right\}} \quad (10) \end{aligned}$$

and then by solving for  $U = \widehat{\Pr}(T \leq t | J_N = \check{j}, J_C = j', Z(t') = Z)$ . The sampled path is completed once state  $De$  is sampled or state  $Di$  is sampled and the next sampled state is again  $Di$ , or after sampling 9 states, whichever comes first. We set the maximum number of transitions to 9 as observed in our dataset (see eTableS1).

## 1.6 Predictions at the Patient Level - Technical Details

We consider the following three types of predictions. Type A is prediction at time of hospitalization, Type B is prediction at the entrance to any new clinical state, and prediction Type C is done during the stay at a certain state. Let  $Z(t)$  consist of age, sex, clinical state at time of hospitalization, the cumulative number of days in hospital **up to the entrance to the current state**, an indicator variable equal to 1 if previously visited Critical state and 0 otherwise, and the interactions of each of these covariates with age.

**Type A.** Given age =  $a$ , sex =  $s$  ( $s$  is either 1 or 0) and state at time of hospitalization  $j^*$ , the vector of covariates for prediction at time of hospitalization is given by

$$Z(t) = Z(0) = \{a, s, I(j^* = M), I(j^* = S), 0, 0, a \cdot s, a \cdot I(j^* = M), a \cdot I(j^* = S), 0, 0\}$$

and Eq's (7) and (8) provide the estimated probabilities of the next state  $j$  and the probability of transitioning by day  $t$  given the transition  $j^* \rightarrow j$  and  $Z(0)$ .

**Type B.** Given age =  $a$ , sex =  $s$ , state at hospitalization  $j^*$ , the patient now entered state  $j'$ , the cumulative number of days in hospital up to the entrance to the current state equals  $t'$ , the vector of covariates for predictions is

$$Z(t') = \{a, s, I(j^* = M), I(j^* = S), t', W, a \cdot s, a \cdot I(j^* = M), a \cdot I(j^* = S), a \cdot t', a \cdot W\}$$

where  $W = 1$  if previously visited  $C$ , and 0 otherwise. Hence, Eq's (9) and (10) provide the estimated probabilities of the next state  $j$  and the probability of transitioning by day  $t$  given the transition  $j^* \rightarrow j'$  and  $Z(t')$ .

**Type C.** Given  $Z(t')$  as in Type B, and given that the patient is at state  $j'$  for already  $d$  days, the following are the updated predictions where we take into account the  $d$  days in current state but there is no change in the vector of covariates  $Z(t')$ . Specifically, the next state probability  $p_{j|j',Z,d}$ ,  $j = 1, \dots, K_{j'}$ , is given by

$$p_{j|j',Z,d} = \frac{\sum_{t'+d < t_m \leq \tau_{j',j}} \exp\left(\widehat{\beta}_{j',j}^T Z\right) \widehat{\lambda}_{0j',j}(t_m) \exp\left\{-\sum_{k=1}^{K_{j'}} \widehat{\Lambda}_{0j',k}(t_{m-1}) \exp\left(\widehat{\beta}_{j',k}^T Z\right)\right\}}{\sum_{j^{**}=1}^{K_{j'}} \sum_{t'+d < t_m \leq \tau_{j',j^{**}}} \exp\left(\widehat{\beta}_{j',j^{**}}^T Z\right) \widehat{\lambda}_{0j',j^{**}}(t_m) \exp\left\{-\sum_{k=1}^{K_{j'}} \widehat{\Lambda}_{0j',k}(t_{m-1}) \exp\left(\widehat{\beta}_{j',k}^T Z\right)\right\}},$$

where summations are over the observed event times of the respective transition. Given the new sampled state, denoted by  $\check{j}$ , the time to be spent at  $j'$  is predicted by

$$\begin{aligned} & \widehat{\Pr}(T \leq t | J_N = \check{j}, J_C = j', Z(t') = Z, d) \\ &= \frac{\sum_{t'+d < t_m \leq t} \exp\left(\widehat{\beta}_{j',\check{j}}^T Z\right) \widehat{\lambda}_{0j',\check{j}}(t_m) \exp\left\{-\sum_{k=1}^{K_{j'}} \widehat{\Lambda}_{0j',k}(t_{m-1}) \exp\left(\widehat{\beta}_{j',k}^T Z\right)\right\}}{\sum_{t'+d < t_m \leq \tau_{j',\check{j}}} \exp\left(\widehat{\beta}_{j',\check{j}}^T Z\right) \widehat{\lambda}_{0j',\check{j}}(t_m) \exp\left\{-\sum_{k=1}^{K_{j'}} \widehat{\Lambda}_{0j',k}(t_{m-1}) \exp\left(\widehat{\beta}_{j',k}^T Z\right)\right\}}. \end{aligned}$$

## 1.7 Weighted Bootstrap Standard Error for Prediction at the Subject Level

Denote the total number of patients in the training data  $n$ . Our goal is estimating the standard error (SE) of predictions of a new patient with baseline covariate  $X^o$ . The following is a weighted bootstrap procedure (Kosorok, 2007) for SE estimation of our proposed MC-based estimators:

1. Sample  $n$  weight values from an exponential distribution with mean 1, and assign a weight value to each patient in the training sample.
2. Estimate the six Cox PH models (1)–(6) with the weights sampled in Step 1.
3. Given  $X^o$ , sample 20,000 MC paths, and based on the 20,000 paths compute all the desired quantities according to Section 1.4.
4. Repeat Steps 1–3  $B$  times.

The empirical variances of the  $B$  estimates are the weighted bootstrap SEs estimates. For example, the empirical variance of the  $B$  death probability estimates is the SE estimate of the estimated death probability of this new patient.

## 1.8 Prediction at the Health-System Level

As described above, for prediction at the patient level, for any given vector of covariates one should run a large number of MC paths, summarize the MC runs and obtain the distributions of LOS in hospital, of LOSCS, etc. Predictions at the hospital level for Snapshot, Arrival or Snapshot plus Arrival (see Section 1.3 for details) require a different MC approach, as follows:

1. Sample one hospitalization path for each patient at the starting date for Snapshot patients and at the patient hospitalization date for Arrival patients.
2. Summarize the paths over all the patients during the predefined period. For example, count the number of patients in the hospital at each day.

3. Repeat Steps 1–2 above a large number of times (e.g. 10,000), and summarize over these repeats. For example, get the mean or various quantiles of the number of patients in the hospital at each day.

## 2 Results

Data analysis was conducted in R (R Core Team, 2020). Table S2 – Table S4 provide the regression coefficients of each of the transition models (1)–(6). The following are summaries of the various MC predictions.

### 2.1 Prediction at the Patient Level

Table S5 provides death probabilities for various patient types defined by sex, age and state at time of hospitalization. Prediction is based on 20,000 MC paths for each patient type along with weighted-bootstrap 95% confidence intervals. As expected, death probability increases with age and with state severity at time of hospitalization. Table S6 gives the probability of being at critical state during hospitalization by patient types along with weighted-bootstrap 95% confidence intervals. The 10%, 25%, 50%, 75% and 90% quantiles of LOS in days and weighted-bootstrap standard errors, by patient type are given in Table S7. Quantiles of LOSCS in days, given being in critical state with weighted bootstrap standard errors are presented in Table S8 by patient type. Plots of the cumulative distribution function of LOS by patient types are provide in Figure S2. All the above results are based on 20,000 MC paths for the estimates of each patient type, and 500 weighted bootstrap samples, each with 20,000 MC paths, for the standard error estimates for each patient type.

The AUROC and Brier Score results, based on 8-fold cross validation, are presented in Table S10 (more details on the 8-fold cross validation study in the next section). The mean AUROC and Brier Scores estimates for death prediction over the eight held-out subsets are 0.955 (SE=0.035) and 0.043 (SE=0.011); the respective AUROC and Brier score of predicting critical clinical state visit are 0.880 (SE=0.040) and 0.049 (SE=0.013).

## 2.2 Prediction at the Health System Level - Random Subset of Patients 8-fold Cross Validation

The entire dataset was randomly partitioned into 8 groups of about 330 patients each. Each time the model was trained with one group omitted (held-out), and our prediction tool was used to provide predictions for the patients of the held-out group. We demonstrate the results of one held-out random group in Figure S3 for the arrival process and two snapshots, at April 1st and 15th. Evidently, our prediction tool performs very well in terms of absolute error. Similar conclusions are obtained from Figure S4 which provides the summary over the 8 held-out groups. Table S9 presents the mean absolute errors (MAE) of each held-out group and over the eight groups. MAE is defined as the mean of the absolute daily-based differences between observed and predicted number of patients; the means are over 64, 32 and 18 days, for the Arrival and the two Snapshot settings, respectively. “ALL” (in Table S9) refers to MAE between the mean curves of the estimated and predicted curves of the 8 held-out random groups, and “Mean” (SE) are the means and SEs of the 8 MAEs. The results show excellent prediction performances with small mean MAE. In particular, 4.72 (SE=1.07) and 1.68 (SE=0.40) for LOS and LOSCS of Arrival; 3.15 (SE=1.20) and 1.47 (SE=0.56) for LOS and LOSCS of April 1st Snapshot; and 3.13 (SE=1.07) and 1.98 (SE=0.93) for LOS and LOSCS of April 15th Snapshot.

## 2.3 Prediction at the Health System Level - Hospital Holdout

We further evaluate the model by training on a sample where patients from each hospital in turn are held-out and not included in the training dataset. Figure S5 and Figure S6 demonstrate our ability to predict for the two hospitals with the largest patient population in our sample, hospitals H5 and H7 (we were asked to avoid identifying the hospital names). Evidently, load predictions for H5 are satisfactory, but not so for H7. It shows that when using our model for predicting at the hospital level, it is preferable to include patients from the predicted hospital in the training data thus avoiding possible hospital-specific biases. Table S11 and Table S12 show the mean absolute error, ROC AUC and Brier Scores for predicting death and visiting critical state for each hospital. In some hospitals, the number of deceased or number of patients with visits at Critical are very small, so results should



be interpreted with caution.

## 2.4 Prediction at the Health System Level - Hypothetical Scenarios

Assume we would like to predict the hospitalized load in a certain health-care system in a given period of time using the Snapshot plus Arrival approach (see Section 1.3 for details). Three hypothetical scenarios were constructed based on the observed arrival process of a random hold-out sample of size 330 (specifically, we used the first random subset described in Section 2.2 and Figure S3):

1. **“Younger”**: patients of age 60 and above within the held-out sample were replaced by patients of ages between 40–50 with probability 2/3, and between 50–60 with probability 1/3. Given the age group of a new patient, the specific age, sex and clinical state at time of hospitalization were sampled based on the distribution of Israeli COVID-19 patients.
2. **“Milder”**: patients at the critical clinical state at time of hospitalization were left at the critical state or replaced by Severe or Moderate patients, each with probabilities 1/3. Given the state at time of hospitalization of a new patient, the specific age and sex were sampled based on the distribution of Israeli COVID-19 patients.
3. **“Elder Care Nursing Home Outbreak”**: On the 5th week from the beginning of the arrival process, and only for this week, the number of patients at age 70 and above was multiplied by four. Age and sex of the new patients were sampled based on the Israeli population distribution, and the state at time of hospitalization was sampled based on the distribution of Israeli COVID-19 patients.

The model was trained by the data not including the random held-out sample, and prediction was performed with 10,000 MC paths as described in Section 1.8. The results are presented in Figure S7 as well as in Figure 2 of the main paper. Table S13 (same as Table 3 of main paper) shows the number of observed death based on the actual data of the held-out sample, versus the expected number of deaths for each of the above hypothetical scenarios. The high similarity between the observed and expected number of deaths

demonstrate that our proposed model is well calibrated. Under the “Younger” scenario the number of deaths decreases dramatically, the decrease is moderate under the “Milder” scenario, and as expected, an outbreak at elder care nursing home yields a substantial increase in number of deaths.

Table S1: Summary of the observed hospitalization course (observed paths): Di - Discharged, M/S - Moderate/Severe, C - Critical, De - Deceased. A patient enters the hospital at a moderate, severe or critical clinical state, and can move among the transient clinical states during the course of hospitalization. The longest observed path consists of 9 transitions.

	path	frequency
1	M/S	148
2	M/S Di	1977
3	M/S Di M/S	19
4	M/S Di M/S Di	68
5	M/S Di M/S Di M/S	1
6	M/S Di M/S Di M/S Di	5
7	M/S Di M/S Di M/S Di M/S Di M/S Di	1
8	M/S Di M/S C	2
9	M/S Di M/S De	2
10	M/S Di C	1
11	M/S Di C M/S Di	1
12	M/S C	49
13	M/S C Di	4
14	M/S C M/S	25
15	M/S C M/S Di	61
16	M/S C M/S Di M/S Di	1
17	M/S C M/S C	8
18	M/S C M/S C M/S	4
19	M/S C M/S C M/S Di	13
20	M/S C M/S C M/S Di M/S	1
21	M/S C M/S C M/S C	1
22	M/S C M/S C M/S C M/S	1
23	M/S C M/S C M/S C M/S C	1
24	M/S C M/S C M/S C De	1
25	M/S C M/S C De	3
26	M/S C M/S De	2
27	M/S C De	64
28	M/S De	44
29	C	42
30	C Di	6
31	C M/S	12
32	C M/S Di	33
33	C M/S Di M/S	1
34	C M/S C	3
35	C M/S C M/S	2
36	C M/S C M/S Di	6
37	C M/S C M/S C	1
38	C M/S C M/S C M/S	2
39	C M/S C M/S C M/S Di	2
40	C M/S C M/S C M/S C	1
41	C M/S C M/S C De	2
42	C M/S C M/S De	1
43	C M/S C De	3
44	C M/S De	4
45	C De	74

Table S2: Results of Cox survival analysis models of transitions from Critical state: STH: state at time of hospitalization (Moderate/Severe/Critical); HistCrt equals 1 if visited Critical state previously; Cum. Days is the number of days in hospital at entry to current state. The reported values are the regression coefficients (robust SE, p-value if smaller than 0.05). Results are based on 460 state visits (a patient can visit the state multiple times). Next states: 140 to Deceased state, 220 to Moderate/Severe state, and 10 to Discharged state.

	Transition to Deceased estimate (SE, pvalue)	Transition to Moderate/Severe estimate (SE, pvalue)
Age	0.022 (0.023)	0.006 (0.009)
Sex (Male)	-3.156 (1.329, 0.018)	0.278 (0.614)
STH (Severe)	-0.799 (1.841)	-0.471 (0.775)
STH (Critical)	-1.410 (1.761)	0.543 (0.758)
Cum. Days	0.059 (0.253)	0.057 (0.078)
HistCrt (yes)	3.499 (3.921)	3.180 (1.451, 0.028)
Age:sex (Male)	0.037 (0.017, 0.028)	-0.011 (0.009)
Age:STH (Severe)	0.012 (0.024)	0.006 (0.011)
Age:STH (Critical)	0.021 (0.022)	-0.011 (0.011)
Age:Cum. Days	-0.0008 (0.003)	-0.0008 (0.001)
Age:HistCrt (yes)	-0.055 (0.046)	-0.030 (0.019)

Table S3: Results of Cox survival analysis models of transitions from Moderate/Severe state: STH: state at time of hospitalization (Moderate/Severe/Critical); HistCrt equals 1 if visited Critical state previously; Cum. Days is the number of days in hospital at entry to current state. The reported values are the regression coefficients (robust SE, p-value if smaller than 0.05). Results are based on 2771 state visits (a patient can visit in the state multiple times). Next states: 53 to Deceased state, 295 to Critical state, and 2233 to Discharged state. Some covariates are not used in some of the models, see 1.1.

	Transition to Deceased estimate (SE, pvalue)	Transition to Critical estimate (SE, pvalue)	Transition to Discharged estimate (SE, pvalue)
Age	0.103 (0.026, 0.0000)	0.029 (0.006, 0.000)	-0.015 (0.002, 0.000)
Sex (Male)	-3.039 (2.351)	0.045 (0.531)	-0.307 (0.145, 0.034)
STH (Severe/Critical)	4.278 (2.544)	-	-
STH (Severe)	-	1.945 (0.589, 0.001)	0.205 (0.186)
STH (Critical)	-	1.275 (1.710)	0.598 (0.899)
Cum. Days	-0.872 (0.532)	0.010 (0.070)	-0.010 (0.027)
HistCrt (yes)	-	1.643 (1.301)	-0.183 (0.660)
Age:sex (Male)	0.037 (0.028)	0.005 (0.007)	0.005 (0.002, 0.028)
Age:STH(Severe/Critical)	-0.037 (0.030)	-	-
Age:STH (Severe)	-	-0.010 (0.008)	-0.009 (0.003, 0.002)
Age:STH (Critical)	-	-0.003 (0.0M/S)	-0.0132 (0.014)
Age:Cum. Days	0.010 (0.006)	0.000 (0.0009)	0.0002 (0.0004)
Age:HistCrt (yes)	-	-0.016 (0.018)	-0.003 (0.010)

Table S4: Results of Cox survival analysis models of transition from Discharged state to Moderate/Severe state: STH: state at time of hospitalization (Moderate vs. Severe/Critical); Cum. Days is the number of days in hospital at entry to current state. The reported values are the regression coefficients (robust SE, p-value if smaller than 0.05). Results are based on 1820 state visits (a patient can visit in the state multiple times). Next states: 0 at Deceased state, 2 at Critical state, and 103 at Moderate/Severe state.

	estimate (SE, pvalue)
Age	0.043 (0.010, 0.0000)
Sex (Male)	0.294 (0.763)
STH (Severe/Critical)	0.648 (1.525)
Cum. Days	0.287 (0.081, 0.0004)
Age:sex (Male)	0.0017 (0.012)
Age:STH (Severe/Critical)	0.007 (0.022)
Age:Cum. Days	0.003 (0.001, 0.0099)

Table S5: Death probability by patient type (state at time of hospitalization, age, sex) based on 20,000 MC paths for each patient type (weighted bootstrap 95% confidence interval).

Patient Type	Male	Female
Moderate, 15	0.000 (0.000,0.002)	0.001 (0.000,0.004)
Moderate, 25	0.001 (0.000,0.003)	0.002 (0.000,0.006)
Moderate, 35	0.002 (0.000,0.005)	0.004 (0.000,0.009)
Moderate, 45	0.003 (0.000,0.007)	0.007 (0.000,0.014)
Moderate, 55	0.009 (0.00,0.02)	0.013 (0.00,0.02)
Moderate, 65	0.022 (0.01,0.03)	0.026 (0.01,0.04)
Moderate, 75	0.058 (0.03,0.09)	0.053 (0.03,0.08)
Moderate, 85	0.151 (0.09,0.21)	0.122 (0.08,0.17)
Severe, 15	0.005 (0.00,0.01)	0.009 (0.00,0.03)
Severe, 25	0.010 (0.00,0.03)	0.017 (0.00,0.05)
Severe, 35	0.016 (0.00,0.04)	0.027 (0.00,0.06)
Severe, 45	0.023 (0.00,0.06)	0.046 (0.00,0.09)
Severe, 55	0.043 (0.00,0.09)	0.075 (0.01,0.14)
Severe, 65	0.096 (0.04,0.15)	0.126 (0.04,0.21)
Severe, 75	0.214 (0.15,0.28)	0.217 (0.13,0.31)
Severe, 85	0.443 (0.32,0.56)	0.389 (0.29,0.49)
Critical, 15	0.023 (0.00,0.11)	0.061 (0.00,0.22)
Critical, 25	0.043 (0.00,0.15)	0.099 (0.00,0.28)
Critical, 35	0.069 (0.00,0.19)	0.153 (0.00,0.34)
Critical, 45	0.083 (0.00,0.22)	0.224 (0.00,0.42)
Critical, 55	0.153 (0.04,0.27)	0.299 (0.11,0.49)
Critical, 65	0.299 (0.18,0.42)	0.414 (0.26,0.57)
Critical, 75	0.546 (0.43,0.66)	0.549 (0.43,0.67)
Critical, 85	0.829 (0.74,0.91)	0.754 (0.65,0.86)

Table S6: The probability of being at critical state during hospitalization by patient type (state at time of hospitalization, age, sex) based on 20,000 MC paths for each type (weighted bootstrap 95% confidence interval).

Patient Type	Male	Female
Moderate, 15	0.011 (0.00,0.02)	0.008 (0.00,0.01)
Moderate, 25	0.016 (0.01,0.02)	0.011 (0.00,0.02)
Moderate, 35	0.025 (0.02,0.03)	0.019 (0.01,0.03)
Moderate, 45	0.037 (0.02,0.05)	0.029 (0.02,0.04)
Moderate, 55	0.059 (0.05,0.07)	0.041 (0.03,0.06)
Moderate, 65	0.085 (0.07,0.10)	0.061 (0.04,0.08)
Moderate, 75	0.129 (0.11,0.15)	0.099 (0.07,0.13)
Moderate, 85	0.179 (0.14,0.22)	0.134 (0.09,0.19)
Severe, 15	0.060 (0.02,0.10)	0.045 (0.00,0.10)
Severe, 25	0.084 (0.04,0.13)	0.067 (0.01,0.13)
Severe, 35	0.127 (0.08,0.18)	0.091 (0.03,0.16)
Severe, 45	0.175 (0.12,0.23)	0.131 (0.07,0.20)
Severe, 55	0.241 (0.19,0.29)	0.185 (0.13,0.24)
Severe, 65	0.319 (0.27,0.37)	0.256 (0.20,0.31)
Severe, 75	0.404 (0.35,0.46)	0.323 (0.27,0.38)
Severe, 85	0.467 (0.39,0.56)	0.385 (0.31,0.46)

Table S7: Quantiles of length of stay in days, by patient type (sex, age and state at time of hospitalization), based on 20,000 MC paths for each patient type (weighted bootstrap standard error).

Patient Type	10%	25%	50%	75%	90%
Male, 15, Moderate	1 (0.37)	3 (0.37)	5 (0.37)	8 (0.53)	13 (0.92)
Male, 25, Moderate	2 (0.49)	3 (0.00)	5 (0.45)	9 (0.47)	14 (0.88)
Male, 35, Moderate	2 (0.41)	3 (0.00)	6 (0.19)	10 (0.48)	16 (0.95)
Male, 45, Moderate	2 (0.01)	3 (0.17)	6 (0.19)	11 (0.49)	18 (0.97)
Male, 55, Moderate	2 (0.00)	4 (0.33)	7 (0.17)	12 (0.58)	21 (0.69)
Male, 65, Moderate	2 (0.00)	4 (0.00)	7 (0.50)	13 (0.52)	24 (1.06)
Male, 75, Moderate	2 (0.00)	4 (0.48)	8 (0.50)	15 (0.66)	28 (1.44)
Male, 85, Moderate	2 (0.32)	5 (0.49)	8 (0.54)	16 (0.94)	29 (2.05)
Male, 15, Severe	1 (0.28)	3 (0.50)	5 (0.58)	8 (0.92)	14 (2.49)
Male, 25, Severe	1 (0.50)	3 (0.20)	6 (0.56)	10 (1.07)	18 (3.14)
Male, 35, Severe	2 (0.29)	3 (0.39)	6 (0.52)	12 (1.29)	25 (3.54)
Male, 45, Severe	2 (0.00)	4 (0.27)	8 (0.56)	16 (1.59)	36 (4.26)
Male, 55, Severe	2 (0.00)	4 (0.49)	9 (0.69)	21 (1.45)	42 (2.76)
Male, 65, Severe	2 (0.49)	5 (0.46)	11 (0.88)	26 (2.01)	45 (1.62)
Male, 75, Severe	3 (0.10)	6 (0.36)	12 (0.10)	28 (2.08)	47 (1.75)
Male, 85, Severe	3 (0.26)	6 (0.47)	10 (0.10)	23 (2.77)	42 (5.89)
Male, 15, Critical	6 (1.21)	9 (2.22)	16 (4.09)	26 (6.87)	41 (6.60)
Male, 25, Critical	6 (1.16)	11 (2.13)	19 (3.78)	31 (6.34)	42 (4.79)
Male, 35, Critical	7 (1.05)	13 (1.92)	22 (3.39)	37 (5.17)	45 (3.03)
Male, 45, Critical	8 (0.92)	14 (1.79)	25 (3.04)	42 (3.51)	47 (2.08)
Male, 55, Critical	8 (0.95)	15 (1.78)	28 (2.49)	44 (2.55)	48 (1.65)
Male, 65, Critical	6 (0.69)	13 (1.58)	26 (2.39)	45 (1.79)	51 (1.76)
Male, 75, Critical	3 (0.79)	8 (0.86)	20 (2.08)	40 (4.71)	48 (1.85)
Male, 85, Critical	2 (0.47)	4 (0.83)	9 (1.25)	21 (3.09)	37 (5.84)
Female, 15, Moderate	1 (0.00)	2 (0.20)	4 (0.24)	7 (0.52)	10 (0.87)
Female, 25, Moderate	1 (0.10)	2 (0.50)	5 (0.50)	8 (0.54)	12 (0.88)
Female, 35, Moderate	1 (0.40)	3 (0.00)	5 (0.34)	9 (0.55)	14 (0.86)
Female, 45, Moderate	2 (0.31)	3 (0.00)	6 (0.17)	10 (0.50)	17 (0.97)
Female, 55, Moderate	2 (0.00)	3 (0.50)	7 (0.37)	12 (0.49)	20 (1.04)
Female, 65, Moderate	2 (0.00)	4 (0.00)	8 (0.46)	13 (0.49)	22 (1.17)
Female, 75, Moderate	2 (0.22)	4 (0.49)	9 (0.49)	15 (0.78)	26 (1.52)
Female, 85, Moderate	3 (0.39)	5 (0.37)	9 (0.51)	17 (1.15)	29 (1.85)
Female, 15, Severe	1 (0.00)	2 (0.22)	4 (0.48)	7 (0.84)	11 (1.92)
Female, 25, Severe	1 (0.20)	3 (0.49)	5 (0.53)	8 (0.87)	14 (2.34)
Female, 35, Severe	2 (0.47)	3 (0.00)	6 (0.49)	10 (1.07)	20 (2.54)
Female, 45, Severe	2 (0.10)	4 (0.46)	7 (0.47)	13 (1.10)	25 (2.59)
Female, 55, Severe	2 (0.00)	4 (0.17)	8 (0.54)	17 (1.22)	31 (2.54)
Female, 65, Severe	3 (0.49)	5 (0.33)	10 (0.62)	21 (1.34)	39 (3.14)
Female, 75, Severe	3 (0.14)	6 (0.36)	11 (0.96)	24 (1.89)	42 (3.29)
Female, 85, Severe	3 (0.50)	6 (0.46)	12 (1.20)	25 (2.75)	37 (4.90)
Female, 15, Critical	5 (1.02)	9 (1.24)	15 (2.38)	26 (4.63)	39 (7.74)
Female, 25, Critical	5 (1.13)	9 (2.17)	16 (4.13)	27 (6.97)	42 (7.02)
Female, 35, Critical	6 (1.00)	10 (1.94)	18 (2.41)	30 (3.59)	42 (6.05)
Female, 45, Critical	5 (1.10)	10 (1.83)	19 (3.17)	32 (5.41)	44 (3.60)
Female, 55, Critical	5 (1.02)	9 (1.65)	20 (2.41)	34 (3.97)	45 (1.91)
Female, 65, Critical	4 (1.03)	8 (1.55)	18 (2.73)	34 (3.96)	45 (1.87)
Female, 75, Critical	3 (0.64)	6 (1.07)	15 (2.91)	31 (4.23)	47 (1.86)
Female, 85, Critical	2 (0.68)	5 (0.91)	9 (1.86)	24 (4.77)	42 (5.62)



Table S8: Quantiles of length of stay in critical state in days, given being in critical, by patient type (sex, age and state at time of hospitalization), based on 20,000 MC paths for each patient type (weighted bootstrap standard error).

Patient Type	10%	25%	50%	75%	90%
Male, 15, Moderate	2 (0.69)	5 (1.43)	10 (2.66)	19 (4.85)	31 (6.48)
Male, 25, Moderate	2 (0.64)	5 (1.28)	10 (2.36)	20 (4.25)	32 (4.91)
Male, 35, Moderate	2 (0.56)	5 (1.04)	10 (1.96)	21 (3.34)	30 (4.10)
Male, 45, Moderate	2 (0.49)	6 (0.92)	12 (1.83)	22 (2.78)	32 (3.11)
Male, 55, Moderate	3 (0.49)	5 (0.81)	11 (1.24)	22 (1.84)	33 (2.31)
Male, 65, Moderate	2 (0.44)	5 (0.70)	12 (1.21)	21 (1.83)	32 (1.94)
Male, 75, Moderate	2 (0.14)	4 (0.56)	11 (1.15)	20 (1.69)	30 (2.50)
Male, 85, Moderate	2 (0.48)	4 (0.67)	9 (1.45)	17 (2.37)	27 (3.07)
Male, 15, Severe	3 (1.07)	7 (2.37)	14 (4.81)	26 (6.84)	36 (6.71)
Male, 25, Severe	3 (0.95)	6 (2.03)	14 (3.92)	25 (5.67)	37 (5.47)
Male, 35, Severe	3 (0.79)	7 (1.78)	14 (3.15)	26 (4.55)	37 (4.11)
Male, 45, Severe	3 (0.63)	7 (1.41)	15 (2.46)	26 (3.40)	36 (3.07)
Male, 55, Severe	3 (0.56)	7 (1.87)	15 (1.72)	25 (2.45)	34 (2.25)
Male, 65, Severe	3 (0.40)	6 (0.98)	14 (1.49)	24 (2.17)	33 (2.13)
Male, 75, Severe	3 (0.50)	6 (0.76)	13 (1.27)	23 (1.75)	31 (2.01)
Male, 85, Severe	2 (0.50)	4 (0.69)	10 (1.68)	19 (2.48)	28 (2.68)
Male, 15, Critical	2 (0.62)	5 (1.45)	11 (2.96)	19 (4.71)	30 (6.37)
Male, 25, Critical	3 (0.64)	6 (1.38)	12 (2.55)	23 (4.09)	33 (5.56)
Male, 35, Critical	3 (0.61)	7 (1.24)	14 (2.26)	25 (3.28)	37 (4.35)
Male, 45, Critical	4 (0.55)	8 (0.96)	16 (1.66)	27 (2.73)	39 (3.23)
Male, 55, Critical	4 (0.63)	8 (1.04)	17 (1.45)	29 (2.00)	40 (2.67)
Male, 65, Critical	4 (0.62)	8 (0.88)	17 (1.29)	30 (2.13)	40 (3.51)
Male, 75, Critical	3 (0.48)	6 (0.63)	14 (1.44)	26 (1.99)	37 (2.85)
Male, 85, Critical	2 (0.43)	4 (0.73)	8 (0.90)	18 (2.33)	30 (2.71)
Female, 15, Moderate	1 (0.85)	4 (1.50)	10 (3.69)	21 (5.66)	28 (7.07)
Female, 25, Moderate	2 (0.66)	4 (1.36)	9 (3.08)	15 (5.04)	22 (6.35)
Female, 35, Moderate	2 (0.52)	4 (0.98)	9 (2.16)	16 (3.81)	25 (5.21)
Female, 45, Moderate	1 (0.57)	3 (0.70)	8 (1.63)	16 (2.84)	24 (4.02)
Female, 55, Moderate	2 (0.46)	3 (0.43)	7 (1.09)	14 (1.74)	24 (2.52)
Female, 65, Moderate	1 (0.47)	3 (0.26)	7 (0.84)	13 (1.37)	21 (1.77)
Female, 75, Moderate	1 (0.48)	3 (0.22)	7 (0.78)	13 (1.27)	22 (1.72)
Female, 85, Moderate	1 (0.43)	3 (0.24)	7 (0.92)	13 (1.48)	21 (2.12)
Female, 15, Severe	3 (1.06)	7 (2.31)	14 (4.52)	26 (6.50)	35 (6.46)
Female, 25, Severe	2 (0.86)	5 (1.91)	12 (3.83)	24 (5.64)	35 (5.89)
Female, 35, Severe	2 (0.74)	5 (1.56)	11 (2.98)	22 (4.73)	32 (5.11)
Female, 45, Severe	2 (0.55)	5 (1.13)	11 (2.34)	20 (3.48)	30 (4.28)
Female, 55, Severe	2 (0.33)	4 (0.67)	9 (1.32)	17 (2.10)	27 (2.77)
Female, 65, Severe	2 (0.32)	4 (0.66)	9 (1.01)	16 (1.58)	25 (2.17)
Female, 75, Severe	2 (0.30)	4 (0.53)	8 (0.98)	15 (1.50)	23 (2.01)
Female, 85, Severe	1 (0.47)	3 (0.35)	7 (1.14)	14 (1.64)	22 (2.21)
Female, 15, Critical	2 (0.80)	5 (1.80)	11 (3.68)	20 (6.36)	32 (7.86)
Female, 25, Critical	2 (0.68)	5 (1.64)	11 (3.15)	21 (5.45)	32 (6.91)
Female, 35, Critical	3 (0.66)	5 (1.34)	11 (2.48)	21 (4.39)	33 (5.62)
Female, 45, Critical	3 (0.60)	5 (0.99)	11 (1.99)	21 (3.48)	32 (4.56)
Female, 55, Critical	3 (0.55)	5 (0.75)	11 (1.46)	20 (2.47)	31 (3.02)
Female, 65, Critical	2 (0.54)	5 (0.70)	10 (1.33)	20 (2.18)	31 (2.89)
Female, 75, Critical	2 (0.54)	5 (0.55)	9 (1.07)	18 (2.07)	28 (2.88)
Female, 85, Critical	2 (0.43)	4 (0.60)	7 (0.84)	15 (2.34)	25 (3.04)

Table S9: Random subset of patients holdout: Mean absolute error (MAE) for predicting number of hospitalized and number of critical patients over each held-out group and over the eight random groups together under the evaluation setups described in subsection 1.3.

Group Number	Arrival		Snapshot		Snapshot	
	All	Critical	Apr 1st, All	Apr 1st, Critical	Apr 15st, All	Apr 15th, Critical
1	3.79	2.07	3.52	1.83	3.78	2.73
2	4.09	2.03	2.03	1.79	1.73	1.97
3	5.99	1.81	4.20	1.19	3.37	3.72
4	6.35	1.58	5.46	0.81	3.39	2.06
5	5.32	1.41	2.19	1.22	4.89	1.17
6	3.48	2.14	2.32	2.27	2.84	2.11
7	3.94	1.04	2.32	0.71	1.63	1.03
8	4.86	1.33	3.14	1.90	3.39	1.04
All	4.11	1.29	2.41	0.75	2.68	1.25
Mean (SE)	4.72 (1.07)	1.68 (0.40)	3.15 (1.20)	1.47 (0.56)	3.13 (1.07)	1.98 (0.93)

Table S10: Random subset of patients holdout: ROC AUC and Brier Score of death prediction and critical-state-visit prediction by held-out group. Critical-state-visit prediction is not including patients started at critical state. The mean ROC AUC and Brier Scores estimates for death prediction over the eight held-out subsets are 0.955 (SE=0.035) and 0.043 (SE=0.011); the respective numbers of visiting-critical prediction are 0.880 (SE=0.040) and 0.049 (SE=0.013).

group number	group size	Death Prediction			Visiting-Critical Prediction		
		number of deceased	AUC	Brier	number in critical (started in critical)	AUC	Brier
1	330	26	0.966	0.047	20 (29)	0.899	0.034
2	331	29	0.936	0.056	23 (28)	0.862	0.048
3	329	19	0.980	0.038	32 (22)	0.958	0.030
4	329	20	0.978	0.028	30 (23)	0.860	0.051
5	331	24	0.977	0.030	34 (23)	0.828	0.053
6	330	28	0.958	0.057	33 (17)	0.904	0.072
7	330	19	0.876	0.038	22 (20)	0.849	0.049
8	330	28	0.971	0.052	32 (22)	0.876	0.055

Table S11: Hospital holdout: Mean absolute error (MAE) for each held-out hospital for predicting number of hospitalized and number of critical patients under the evaluation setups described in subsection 1.3.

Hospital	Number of Patients	All Patients (MAE)	Critical Patients (MAE)	Snapshot Apr 1st All (MAE)	Snapshot Apr 1st Critical (MAE)	Snapshot Apr 15st All (MAE)	Snapshot Apr 15st Critical (MAE)
H1	298	8.51	2.24	3.57	1.44	4.57	1.19
H2	166	6.48	0.82	4.10	0.66	3.83	1.15
H3	142	3.91	1.55	1.57	0.64	1.14	1.29
H4	105	3.78	1.01	1.65	1.96	1.53	1.46
H5	343	5.55	1.67	2.68	1.29	5.74	2.08
H6	111	2.11	0.75	2.02	0.63	2.15	0.92
H7	373	11.44	7.06	7.11	8.58	10.40	7.74
H8	215	5.71	2.61	7.79	1.10	2.41	3.66

Table S12: Hospital holdout: ROC AUC and Brier Score of death prediction and critical-state visit prediction for each held-out hospital. Critical-state-visit prediction does not include patients who started hospitalization at critical state.

Hospital	Number of Patients	Death Prediction			Visiting-Critical Prediction		
		Number of Deceased	AUC	Brier	Number in Critical (started in Critical)	AUC	Brier
H1	298	16	0.856	0.043	22 (18)	0.699	0.045
H2	166	5	0.986	0.020	7 (10)	0.999	0.021
H3	142	11	0.976	0.048	16 (11)	0.917	0.092
H4	105	8	0.946	0.053	8 (4)	0.953	0.052
H5	343	26	0.982	0.044	35 (34)	0.892	0.059
H6	111	8	0.913	0.047	12 (7)	0.801	0.066
H7	373	26	0.970	0.046	43 (27)	0.897	0.046
H8	215	23	0.959	0.039	29 (23)	0.951	0.047

Table S13: Predicted number of deaths (in-hospital mortality) within a random subset of 330 held-out patients: based on Arrival plus Snapshot prediction results of hypothetical scenarios, prediction starts on the 15th day of the observed arrival process. The numbers are the observed and predicted number of deaths for each hypothetical scenario from hospitalization day up to day  $t$  in hospital,  $t = 5, 10, \dots, 35$ .

Day $t$	Observed	Expected	Younger	Milder	NH Outbreak
5	7	6.5	0.6	3.7	8.2
10	16	16.6	1.9	11.7	22.6
15	20	20.4	2.5	15.0	28.3
20	23	22.8	3.0	17.3	32.1
25	24	25.4	3.4	19.7	36.5
30	25	25.9	3.5	20.1	37.0
35	26	26.6	3.7	20.6	37.7

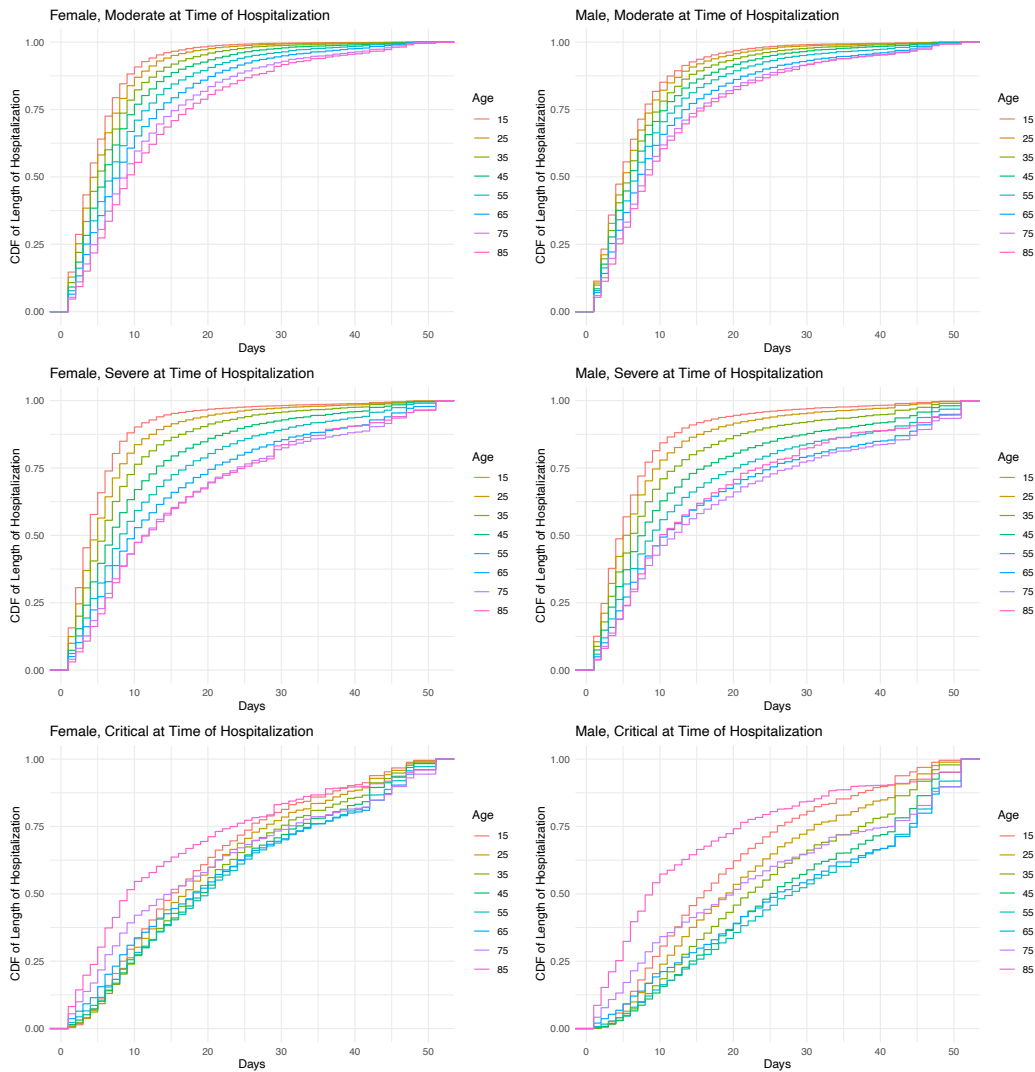


Figure S2: The cumulative distribution function of the length of hospitalization by patient types (sex, state at time of hospitalization and age). Each curve is based on 20,000 MC paths.

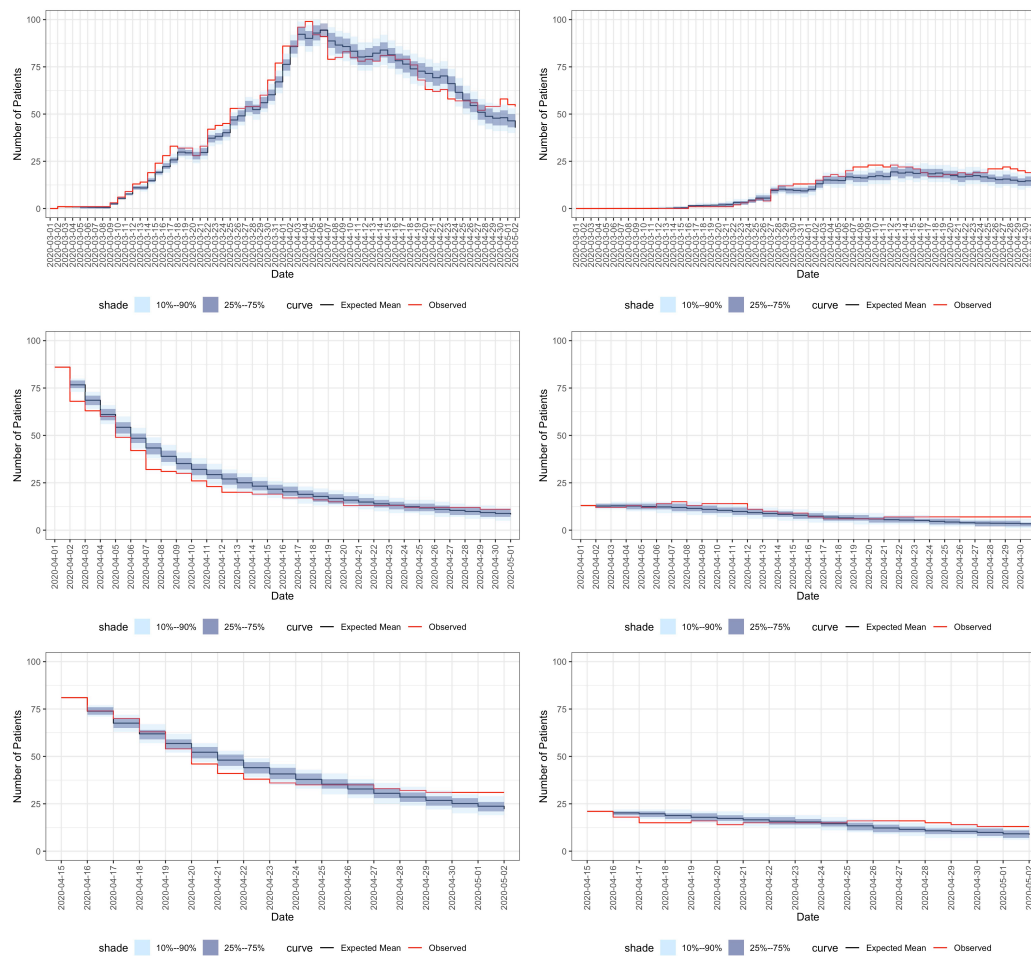


Figure S3: Prediction results of one held-out random group of patients. **Left figures:** utilization predictions for the entire held-out sample. **Right figures:** utilization predictions for critical patients among the held-out sample. **Top figures:** Arrival-type predictions of the entire held-out set based on the observed arrival process. **Middle figures:** Snapshot-type predictions for patients at the hospital on April 1st. **Bottom figures:** Snapshot predictions for patients in the hospital on April 15th. For description of Arrival and Snapshot see Section 1.3.

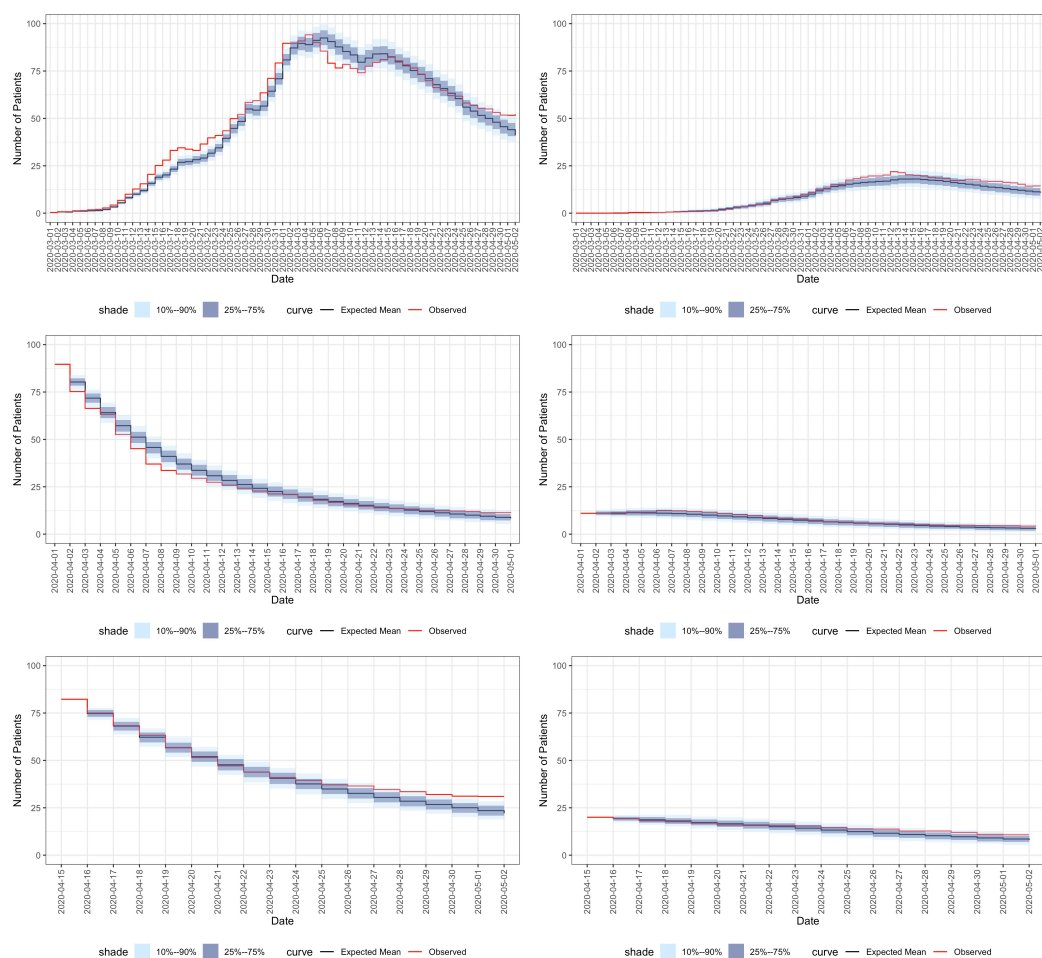


Figure S4: Prediction results summarized over all 8 held-out random groups of patients. **Left figures:** utilization predictions for the entire held-out sample. **Right figures:** utilization predictions for critical patients among the held-out sample. **Top figures:** Arrival-type predictions of the entire held-out set based on the observed arrival process. **Middle figures:** Snapshot-type predictions for patients at the hospital on April 1st. **Bottom figures:** Snapshot predictions for patients in the hospital on April 15th. For description of Arrival and Snapshot see Section 1.3.

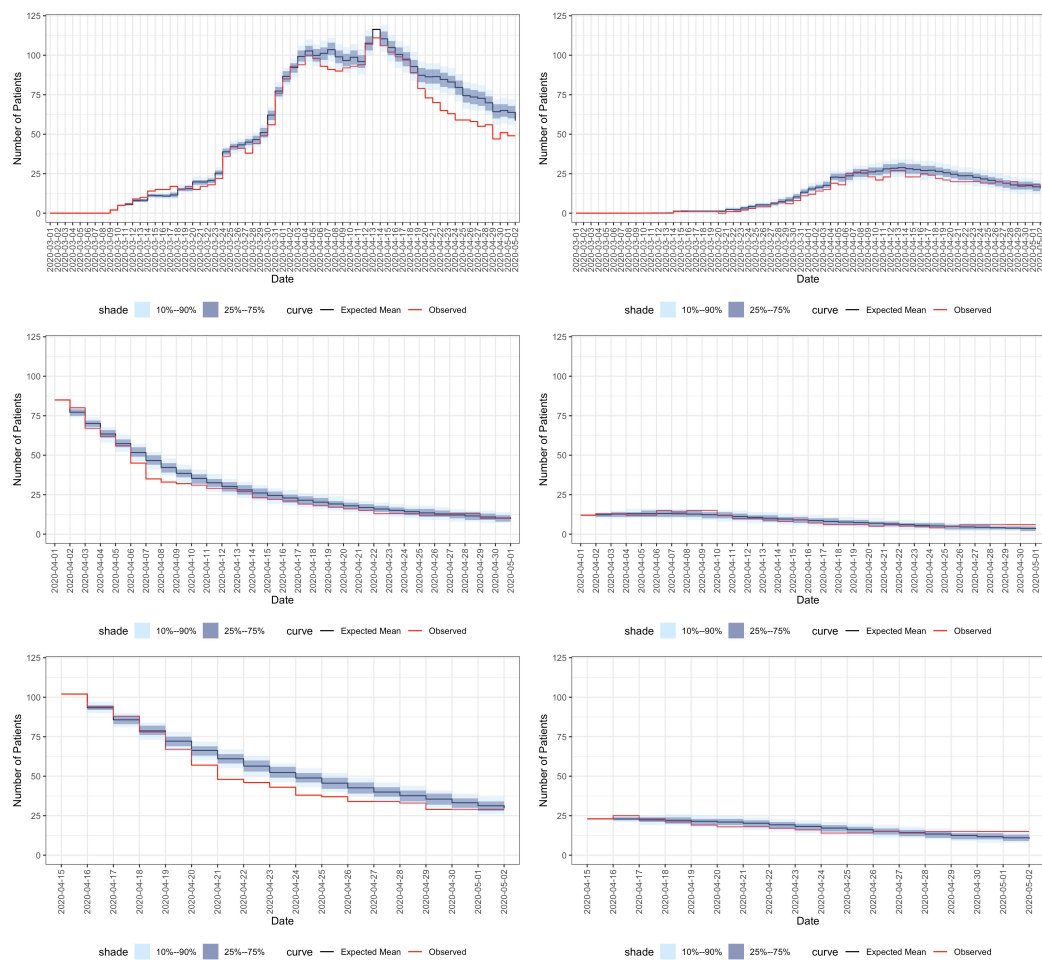


Figure S5: Prediction results - H5 Hospital is held out and predicted based on all other Israeli Hospitals. **Left figures:** utilization predictions for the entire held-out sample. **Right figures:** utilization predictions for critical patients among the held-out sample. **Top figures:** Arrival-type predictions of the entire held-out set based on the observed arrival process. **Middle figures:** Snapshot-type predictions for patients at the hospital on April 1st. **Bottom figures:** Snapshot predictions for patients in the hospital on April 15th. For description of Arrival and Snapshot see 1.3.



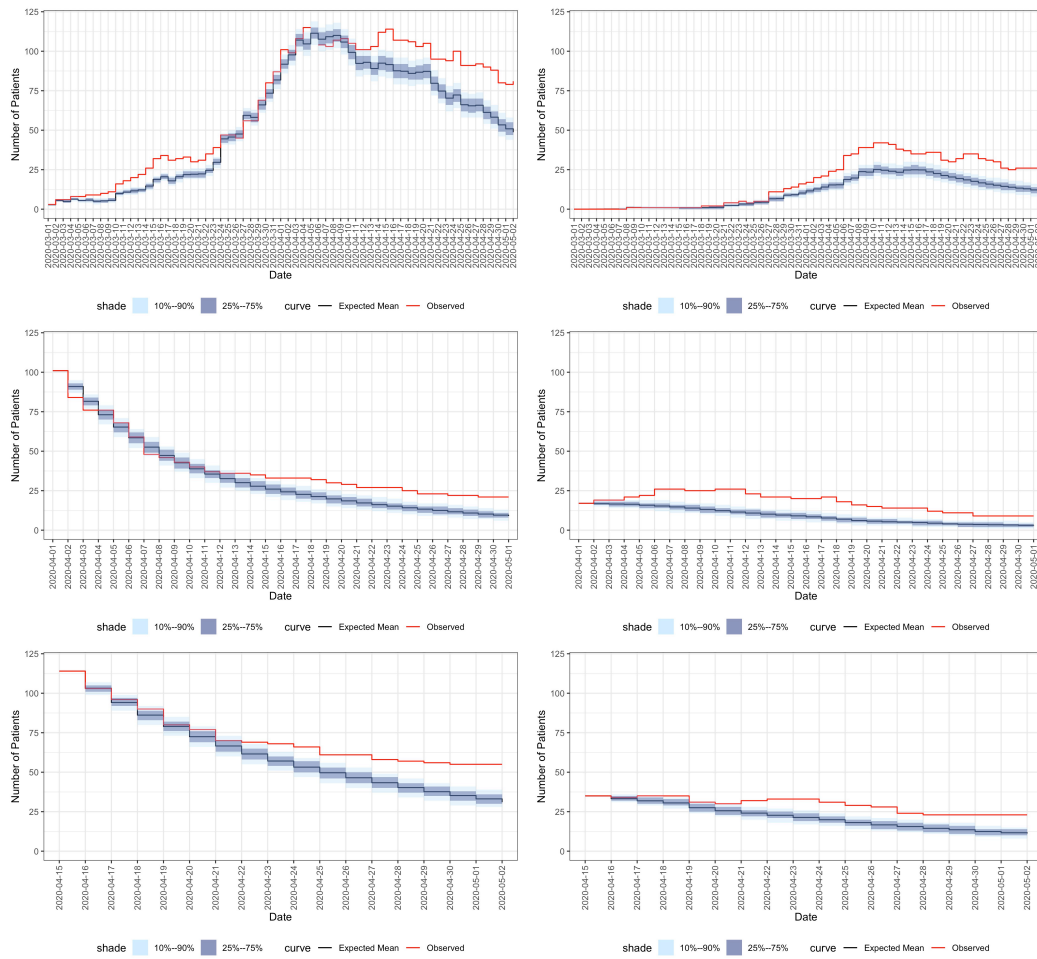


Figure S6: Prediction results - H7 Hospital is held out and predicted based on all other Israeli Hospitals. **Left figures:** utilization predictions for the entire held-out sample. **Right figures:** utilization predictions for critical patients among the held-out sample. **Top figures:** Arrival-type predictions of the entire held-out set based on the observed arrival process. **Middle figures:** Snapshot-type predictions for patients at the hospital on April 1st. **Bottom figures:** Snapshot predictions for patients in the hospital on April 15th. For description of Arrival and Snapshot see 1.3.

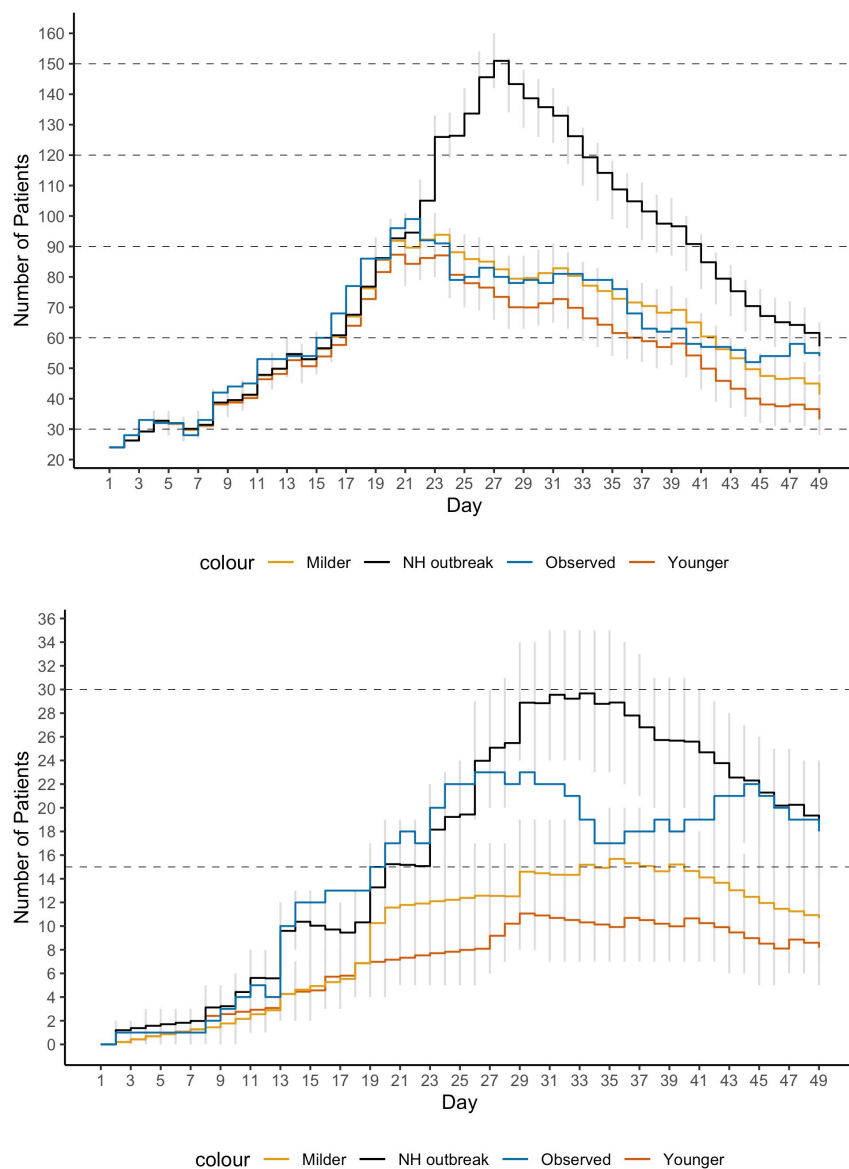


Figure S7: Arrival plus Snapshot prediction results of hypothetical scenarios: 330 random patients were held-out and prediction started on the 15th day of the observed arrival process (denoted as Day 1 in the figures). **Top figure:** utilization predictions based on the entire held-out sample. **Bottom figure:** utilization predictions for critical patients among the held-out sample. Gray vertical lines are point-wise 10%-90% confidence predictions.

## References

- ANDERSEN, P. K. & GILL, R. D. (1982). Cox’s regression model for counting processes: a large sample study. *The annals of statistics* , 1100–1120.
- ANDERSEN, P. K., HANSEN, L. S. & KEIDING, N. (1991). Non-and semi-parametric estimation of transition probabilities from censored observation of a non-homogeneous markov process. *Scandinavian Journal of Statistics* , 153–167.
- HOCKING, T. D. (2020). *WeightedROC: Fast, Weighted ROC Curves*. R package version 2020.1.31.
- KALBFLEISCH, J. D. & PRENTICE, R. L. (2011). *The statistical analysis of failure time data*, vol. 360. John Wiley & Sons.
- KLEIN, J. P. & MOESCHBERGER, M. L. (2006). *Survival analysis: techniques for censored and truncated data*. Springer Science & Business Media.
- KOSOROK, M. R. (2007). *Introduction to empirical processes and semiparametric inference*. Springer Science & Business Media.
- R CORE TEAM (2020). *R: A Language and Environment for Statistical Computing*. R Foundation for Statistical Computing, Vienna, Austria.
- ROBINS, J. M. & FINKELSTEIN, D. M. (2000). Correcting for noncompliance and dependent censoring in an aids clinical trial with inverse probability of censoring weighted (ipcw) log-rank tests. *Biometrics* **56**, 779–788.